(2)

NAVAL POSTGRADUATE SCHOOL
Monterey, California

THESIS

OSCILLATING MICROBUBBLES CREATED BY WATER DROPS FALLING ON FRESH AND SALT WATER: AMPLITUDE, DAMPING AND THE EFFECTS OF TEMPERATURE AND SALINITY.

by

Christopher D. Scofield

June, 1992

Thesis Advisor: Herman Medwin
Co-Advisor: Jeffrey A. Nystuen

REPORT DOCUMENTATION PAGE

Form Approved
OMB No 0704-0188

1a REPORT SECURITY CLASSIFICATION	1b RESTRICTIVE MARKINGS
2a SECURITY CLASSIFICATION AUTHORITY	3 DISTRIBUTION / AVAILABILITY OF REPORT Approved for public release; distribution is unlimited.
2b DECLASSIFICATION / DOWNGRADING SCHEDULE	
4 PERFORMING ORGANIZATION REPORT NUMBER(S)	5 MONITORING ORGANIZATION REPORT NUMBER(S)
6a NAME OF PERFORMING ORGANIZATION: Naval Postgraduate School 6b OFFICE SYMBOL (If applicable): 33	7a NAME OF MONITORING ORGANIZATION: Naval Postgraduate School
6c ADDRESS (City, State, and ZIP Code): Monterey, CA 93943-5000	7b ADDRESS (City, State, and ZIP Code): Monterey, CA 93943-5000
8a NAME OF FUNDING / SPONSORING ORGANIZATION 8b OFFICE SYMBOL (If applicable)	9 PROCUREMENT INSTRUMENT IDENTIFICATION NUMBER
8c ADDRESS (City, State, and ZIP Code)	10 SOURCE OF FUNDING NUMBERS PROGRAM ELEMENT NO / PROJECT NO / TASK NO / WORK UNIT ACCESSION NO

11 TITLE (Include Security Classification) OSCILLATING MICROBUBBLES CREATED BY WATER DROPS FALLING ON FRESH AND SALT WATER: AMPLITUDE, DAMPING AND THE EFFECTS OF TEMPERATURE AND SALINITY

12 PERSONAL AUTHOR(S) Christopher D. Scofield

13a TYPE OF REPORT	13b TIME COVERED	14 DATE OF REPORT (Year, Month, Day)	15 PAGE COUNT
Master's Thesis	FROM _____ TO _____	June 1992	73

16 SUPPLEMENTARY NOTATION The views expressed in this thesis are those of the author and do not reflect the official policy or position of the Department of Defense or U.S. Government.

17 COSATI CODES			18 SUBJECT TERMS (Continue on reverse if necessary and identify by block number)
FIELD	GROUP	SUB-GROUP	Effects of temperature and salinity on the damping constant, pressure and energy of bubbles radiating in water.

19 ABSTRACT (Continue on reverse if necessary and identify by block number)

Recent studies of underwater sound produced by raindrops have identified trapped bubbles as the principle sound source. Two mechanisms have been described, one for small drops (Type I) and one for large drops (Type II). A study of sound produced by large raindrops (Jacobus, 1991) showed that the underwater sound radiated by raindrops is 45% less in salt water (salinity, 35ppt) than in fresh water. The same studies also showed that bubbles radiate more energy as the magnitude of the temperature difference between the drop and surface increases.

These findings are examined in more detail using the pressure decay curve of of both small and large raindrops. Using small raindrops it is shown that bubbles in salt water have a larger damping constant and smaller initial peak pressures than bubbles in fresh water. Reviewing data from Jacobus (1991) for large raindrops, increasing the absolute temperature difference between the drop and bubble showed little effect on the damping constant, but did increase peak pressure. Since the sound energy radiated by a bubble is directly proportional to the peak pressure squared and inversely proportional to the damping constant, the energy radiated by bubbles from raindrops increases with absolute temperature difference and decreases with salinity.

20 DISTRIBUTION / AVAILABILITY OF ABSTRACT	21 ABSTRACT SECURITY CLASSIFICATION
☒ UNCLASSIFIED UNLIMITED ☐ SAME AS RPT ☐ DTIC USERS	Unclassified
22a NAME OF RESPONSIBLE INDIVIDUAL: H. Medwin	22b TELEPHONE (Include Area Code): (408)-624-1775 / 22c OFFICE SYMBOL: PH/Md

DD Form 1473, JUN 86 Previous editions are obsolete

Approved for public release; distribution is unlimited.

Oscillating microbubbles created by water drops falling on fresh and salt water:
Amplitude, damping and the effects of temperature and salinity

by

Christopher D. Scofield
Lieutenant , United States Navy
B.S., Miami University 1986

Submitted in partial fulfillment
of the requirements for the degree of

MASTER OF SCIENCE IN ENGINEERING ACOUSTICS

from the

NAVAL POSTGRADUATE SCHOOL
June 1992

Author: _____
Christopher D. Scofield

Approved by: _____
Herman Medwin, Thesis Advisor

_____
Jeffrey A. Nystuen, Co-Advisor

_____
Anthony A. Atchley, Chairman
Engineering Acoustics Academic Committee

ABSTRACT

Recent studies of underwater sound produced by raindrops have identified trapped bubbles as the principle sound source. Two mechanisms have been described, one for small drops (Type I) and one for large drops (Type II). A study of sound produced by large raindrops (Jacobus, 1991) showed that the underwater sound radiated by the raindrops is 45 % less in salt water (salinity, 35 ppt) than in fresh water. The same studies also showed that bubbles radiate more energy as the magnitude of the temperature difference between the drop and surface increases.

These findings are examined in more detail using the pressure decay curve of both large and small raindrops. Using small raindrops it is shown that bubbles in salt water have a larger damping constant and smaller initial peak pressures than bubbles in fresh water. Reviewing data from Jacobus (1991) for large raindrops, increasing the absolute temperature difference between the drop and bubble showed little effect on the damping constant, but did increase peak pressure. Since the sound energy radiated by a bubble is directly proportional to the peak pressure squared and inversely proportional to the damping constant, the energy radiated by bubbles from raindrops increases with absolute

temperature difference and decreases with salinity.

TABLE OF CONTENTS

ACKNOWLEDGEMENTS

I wish to thank Professor's Herman Medwin and Jeffrey A. Nystuen for their guidance, encouragement and for putting up with me; Capt Kristen A. Dotterway, USAF for her support; Lt. Vance Brahosky, USN for an afternoon of learning word perfect and drinking Sam Adams beer and Lt. Glenn A. Miller USN (no not the same one) for his help in taking data.

Finally, after spending the better part of the last six months studying bubbles produced by raindrops I only have one more question. Does the rain in Spain fall mainly on the plain ?

I. INTRODUCTION

Man has always been driven to explore the unknown and this desire is probably the reason why man has always explored the oceans. One of the tools that can be used to explore the ocean is sound. Knudsen (1948) published measurements of underwater noise and characterized the spectrum in terms of the wind speed. Wenz (1962) discovered that in the frequency range of 1 kHz to 50 kHz the primary contributors to undersea noise are wind and precipitation. Franz (1959) concluded that the underwater sound produced by precipitation was the result of the raindrop impacting on the surface and the oscillations of bubbles which sometimes formed during the splash. Of these two mechanisms, sound energy from the oscillations of the bubbles is usually much greater than the impact sound.

Not all raindrops produce bubbles. Recent studies (Kurgan, 1989; Medwin, et al.,1992) have revealed that small raindrops, ranging in diameter from 0.8 to 1.1 mm, produce bubbles 100% of the time, by a mechanism called Type I, when impact is at normal incidence onto a smooth surface. The same studies also showed that, for small raindrops, the percentage of bubbles produced decreases as the angle of incidence (measured from the normal) of the raindrop increases. Other studies for large raindrops (Snyder,1989; Jacobus,1991)

demonstrated that a different mechanism, Type II, for drops with diameters of 2.2 to 4.6 mm, produces bubbles from zero to 50 or 60 percent of the time. Mid-size drops with diameters of 1.1 to 2.2 mm do not produce bubbles (Medwin, et al.,1992). When bubbles are produced, their oscillations decay exponentially at a rate which is proportional to a damping constant.

Devin (1959) described the damping of pulsating bubbles in freshwater. He summarized the experimental results of others (Meyer, Tamm, Carstensen, Foldy, Bauer, Lauer, Exner, Hampe and Haeske) and stated that the damping of a bubble at resonance in freshwater is due to three types of damping: "thermal damping" which results from the flow of heat energy into the water surrounding the bubble, "radiation damping" which is the loss of energy in the form of spherical sound waves radiated into the surrounding water and "viscous damping" which is caused by the viscous forces of the surrounding liquid exerting an excess pressure on the bubble which results in the dissipation of energy. These experiments did not address other environmental effects which might affect the total energy radiated nor did they address bubbles created by raindrops.

Jacobus (1991) studied the dependence of sound radiation on temperature and concluded that the energy produced by the Type II raindrop mechanism increased as the absolute temperature difference between the water surface and raindrop increased. Other studies by Jacobus dealt with the sound of raindrops splashing in saltwater. These experiments found that the sound produced by large drops is effected by salinity, with an average of 45% less sound energy radiated into saline water compared to fresh water. From these results it was determined that, for large drops, the energy radiated by the bubbles could be given by the equation (Jacobus, 1991)

$$Sound\ Energy = (12.4 + 1.03\ T) \times (Volume - 7) \times (1 - Salinity/77) \quad (1)$$

where energy is in picojoules (pJ), the absolute temperature difference between the drop and the surface T is in degrees centigrade, volume is in microliters and salinity is in parts per thousand (ppt).

All the studies of the effects of changing environmental conditions on the sound of rainfall in water were very broad in scope. While they identified differences, no in-depth studies have been conducted on the way in which the temperature differences or salinity affect pulsating air bubbles in water. The purpose of this thesis is to determine

the actual causes for the differences found by Jacobus by looking at the details of the signal radiated. The actual behavior of the bubble in the water will also be studied with the possible movement during radiation of the bubbles being considered.

Theoretically, salinity and temperature could change the energy radiated by rainfall in a number of ways. One way would be to change the percentage of bubbles produced. Other ways to change the bubble radiation would be by affecting the damping constant or the peak pressure of the bubble. For Type II mechanisms Jacobus (1991) showed that absolute temperature difference between the raindrop and surface had no effect on the percentage of bubbles produced, while Ostwald (1992) showed the percentage of bubbles produced in salt water was comparable to the percentage in freshwater.

This thesis, which will study bubbles produced from both Type I and Type II mechanisms, will first look at the damping constant of bubbles under various conditions. A change in the damping constant would effect the duration of the bubble oscillation and therefore would affect the measured amount of vibrational energy radiated. Next, the peak amplitude pressures of bubbles produced will be examined in an attempt to determine if there is any correlation between the peak pressure and environmental conditions. Finally the results of

these studies will be used to show how the sound energy radiated from bubbles produced by raindrops is affected by salinity and temperature.

II. THEORY

The amount of energy radiated into the water by raindrops can be affected by salinity and temperature in several ways. Recent studies by Jacobus (1991) and Ostwald (1992) show that, for Type II mechanisms, the percentage of raindrops which produce bubbles is independent of the temperature between the raindrop and surface or salinity. This, coupled with the fact that the energy of the impact is significantly less than the energy of the bubble, indicates that most of the effects of salinity and temperature must affect the bubble oscillation. For this reason, this thesis will concentrate on the study of bubble oscillations and not consider the impact.

The bubble behaves like a damped, undriven harmonic oscillator (Medwin and Clay, Appendix A6.1.2,1977). The motion of such an oscillator is described by the equation

$$m d^2x/dt^2 + R_m dx/dt + sx = 0 \qquad (2)$$

where R_m is the mechanical resistance of the system, m is the effective mass, s is the stiffness and the variable x is difference between the bubble radius a and the equilibrium

radius a_o (Pumphrey and Crum,1989). For a bubble, R_m can be represented by the equation (Medwin and Clay, 1976)

$$R_m = 4\pi a^3 \rho \omega \delta. \tag{3}$$

In the above equation ω is the angular frequency, a is the bubble radius, ρ is the density of the water surrounding the bubble (1.03×10^3 kg/m^3) and δ is the damping constant. The effective mass of the bubble is represented by the equation (Medwin and Clay, 1976)

$$m = 4\pi a^3 \rho. \tag{4}$$

A solution of (2) is

$$x = e^{-t/t_o} \sin \omega_o t \tag{5}$$

where ω_o, the angular resonance frequency, can be written

$$\omega = 2\pi f_o. \tag{6}$$

The time it takes the bubble to decay to 1/e of its peak pressure, t_o, can be represented by the equation (Kinsler, Frey, Coppens and Sanders, 1982)

$$t_e = (2m)/R_m. \tag{7}$$

Therefore, combining (7) with (3) and (4),

$$t_e = (8\pi a^3\rho)/(4\pi a^3\rho\omega_o\delta) = 1/(\pi f_o\delta). \tag{8}$$

Rearranging (8) produces the equation for the damping constant

$$\delta = 1/(\pi t_e f_o) \tag{9}$$

where f_o is the resonance frequency. The damping constant is often further broken into three component damping constants at resonance. These three constants are the damping constant due to reradiation δ_r, the damping constant due to thermal conductivity δ_t and the damping constant due to viscosity δ_v. Combining these produces

$$\delta = \delta_r + \delta_t + \delta_v \tag{10}$$

which is another form of the damping constant equation (Medwin and Clay,1976).

The pressure also affects the total energy radiated by the bubble. With respect to (2) and (5), the pressure, p, radiated to a field point by a bubble can be written as

$$p = Pe^{-t/t_o}\sin\omega t \qquad (11)$$

where P is the initial (peak amplitude) pressure of the bubble. Integrating the square of the pressure with respect to time, the energy density radiated by an oscillating bubble to a field point is given by the equation (Kinsler, Frey, Coppens and Sanders, 1982)

$$E = (1/\rho_o c)\int_0^\infty p^2 dt. \qquad (12)$$

Assuming (11), the solution of (12) is

$$E = P^2/(4\pi\rho_o c f_o \delta). \qquad (13)$$

This shows that the energy produced per unit area by a bubble oscillating in water is proportional to the peak pressure squared and inversely proportional to the damping constant.

Because most bubbles formed by rain drops are found near the surface, their radiation is mirrored in the surface and they therefore act as dipole sources (Medwin and Beaky,1989). For a bubble with constant volume displacement V, the dipole pressure can be given by the equation (Clay and Medwin, 1977):

$$P_d = \frac{(i\rho_\lambda \omega V_*)}{(4\pi)} \left(\frac{e^{i(\omega t - kR_1)}}{R_1} - \frac{e^{i(\omega t - kR_2)}}{R_2} \right) \qquad (14)$$

where R_1 and R_2 are the ranges to the dipole sources, ω is the angular frequency, k is the wave number and ρ_λ is the density. V_* is the rate of volume displacement of one of the point sources and can be represented by the equation (Medwin and Beaky, 1989)

$$V_* = 4\pi a^2 U \qquad (15)$$

in which a is the bubble radius and U is the radial velocity amplitude. Simplifying (14) produces (Medwin and Beaky, 1989)

$$P_d = \frac{(k^2 \rho c D \cos\theta)}{4\pi R} \sqrt{1 + \frac{1}{k^2 R^2}} \qquad (16)$$

which shows the pressure of a dipole is proportional to f_o^2 and D, the dipole strength which is given by (Medwin and Beaky, 1989)

$$D = V_s L \tag{17}$$

where L is the distance from bubble center to image center. Therefore, since the peak pressure is actually the dipole pressure a better way to write (13) would be

$$E = \frac{P_d^2}{4\pi\varrho c f_o \delta} \tag{18}$$

where P_o is the dipole pressure developed in (16).

The preceding development assumed that the bubble is fixed in one place. At other times there are indications it may move. When a bubble is close to a free surface its frequency will be higher than when it is away from the surface (Strasburg, 1953). For bubbles that are created at, or very near to the surface, the change of frequency as a result of bubble position can be given by the equation (Medwin and Beaky,1989)

$$f_2 = f_1 F \tag{19}$$

where f_1 is the frequency of the bubble oscillation in free space, f_2 is the frequency at depth z and F, a function of depth, is given by the following equation (Medwin and Beaky, 1989),

$$F = \frac{1}{\sqrt{1-\frac{a}{2z} - (\frac{a}{2z})^4}}. \qquad (20)$$

Since the f_1 and f_2 can be obtained from Computerscope, solving the ratio f_1/f_2 produces a numerical value for F and thus the distance a bubble has moved can be calculated.

In summary, the sound energy radiated by a bubble produced by raindrops could be obtained by integrating (12) over the dipole radiation pattern. It is directly proportional to the square of the pressure (and therefore the dipole strength) and inversely proportional to the damping constant and frequency.

III. THE EFFECT OF SALINITY ON THE DAMPING CONSTANT

A. EXPERIMENT

The drop diameters used for this experiment were 0.83 mm and 0.985 mm, "small" drops by the definition from Medwin et al. (1992). To produce these drops, an Eppendorf digital pipette, which can accurately produce drops ranging in diameter from 0.58 mm to 2.67 mm, was used. In most cases the dropper was held at a height of two meters above the surface, enough to ensure the drops reached a terminal velocity of about 3.6 m/s before impact. In some cases, the dropper height was lowered so that the drops would not reach terminal velocity and bubbles of a wider frequency range would result as shown in Figure 1 (Elmore, Pumphrey and Crum, 1989). Figure 1 shows that the resonance frequency of a bubble is dependent on the diameter of the drop which produces the bubble and the velocity the drop is travelling when it impacts on the surface of the water. The drops landed as close as possible to a point directly above a submerged hydrophone.

Two anechoic tanks were used. For the drops onto salt water, a 1.5 m deep by 1.5 m diameter anechoic tank lined with redwood wedges was used. For the drops onto fresh water, a 3

m x 3 m x 2.9 m deep tank with redwood baffles lining the sides and bottom was used.

An LC-10 hydrophone with a sensitivity of -209 dB ref 1V per μPa with a frequency response of ±1 dB to 100 kHz was used to measure the sound produced by the bubbles. The hydrophone was placed at a depth of either 7.0 cm (salt water) or 7.5 cm (fresh water) and the output fed into an Ithaco 1201 Preamplifier set up as a bandpass filter passing the frequency band from 1 to 30 kHz. The output of the preamplifier was fed into a Krohn-Hite filter (model number 3202R) connected in series and also set up as a bandpass filter passing frequencies from 1 to 30 kHz. The Krohn-Hite was connected to a computer fitted with an RC Electronics analog to digital converter board. A program, called Computerscope, processed the signals, sampling the hydrophone output at a sampling rate of 250 kHz. A signal resulting from a bubble oscillation processed by Computerscope is shown in Figure 2.

The resonance frequency of each bubble was calculated from Computerscope by using a cursor to measure the time between adjacent peaks in the middle of the oscillation and then taking the reciprocal of this time difference. Each bubble oscillation signal was then made into an ASCII file and, using MATLAB, the peaks of its absolute values plotted on a semilog

plot as shown in Figure 3. The slope was drawn through each semilog plot and the time it took the bubble to decay to an amplitude 1/e times its initial peak value measured. This time, denoted t_e, is related to the damping constant δ through the equation

$$\delta = 1/(f_o t_e \pi) \qquad (9)$$

where f_o is the resonance frequency of the bubble.

Only bubbles with visually "clean" oscillations, free from tank reverberation and other noise, were used. A set of 53 data points (22 fresh and 31 salt water) were plotted in comparison to theory (Devin, 1959) in Figures 4 and 5. The frequency range was then divided into 2 kHz bins and the damping constants in these bins were averaged. This was done separately for both the fresh and salt water cases, with the ratio of the averages shown in Figure 6.

B. RESULTS

Figure 4 shows that the experimental damping constants for fresh water are consistent with the theoretical values except between 12-14 kHz. Figure 5 shows that the salt water data points are also consistent with theory, although perhaps higher from 16-18 kHz. In both cases the experimental damping constants increase with frequency, as expected.

Figure 6 shows the ratios of the experimental damping constants for the fresh and salt water after all 53 data points were divided into 2 kHz bins and averaged. In the 14-16 kHz, 16-18 kHz and 20-22 kHz bins, only one fresh water sample was available, and while numerous salt water samples were available for each bin (two for 14-16 kHz, six for 16-18 kHz and two for 20-22 kHz), this detracts from the accuracy of these data points. The frequency bands of 10-12, 12-14 and 22-24 kHz have three, five and three fresh water samples and thirteen, six and two salt water samples respectively and therefore are more accurate. Averaging the ratios of the salt water to fresh water damping constants produced an average of 1.10 with a standard deviation from the mean of 0.085. That is, the salt water damping constant is, on average, 10 percent greater than the damping constant for bubbles of the same frequency in fresh water.

Therefore it appears, as a result of the larger damping constant, that bubbles in salt water have a shorter duration of oscillation than bubbles of the same frequency in fresh water. In accordance with (19), this would effect the sound energy produced by bubbles in salt water, but it would not account for all of the 45% loss noted by Jacobus (1991).

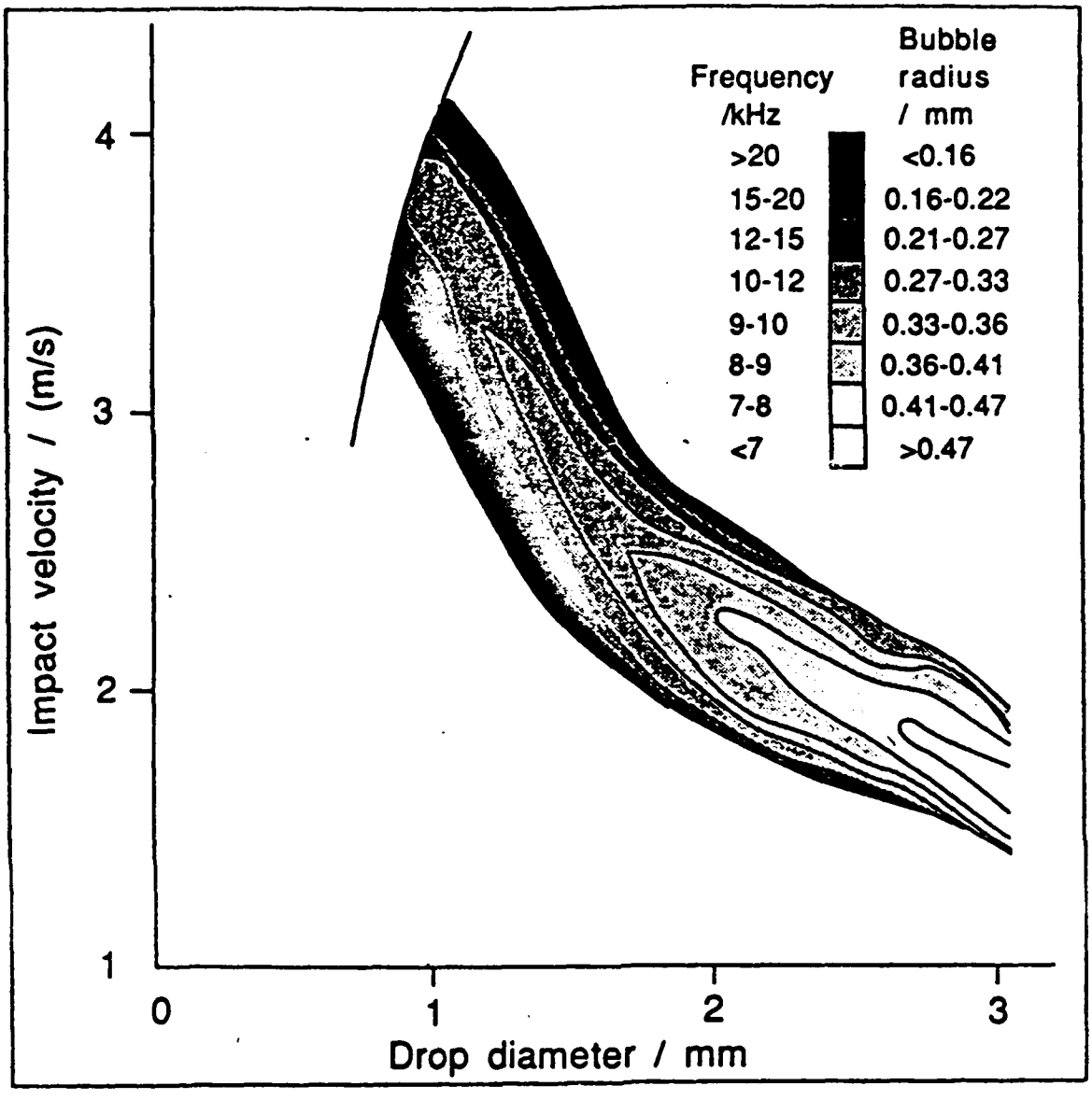

Figure 1. Dependence of bubble resonant frequency on impact, velocity and drop diameter: This figure is taken from Elmore, Pumphrey and Crum (1989). The different shades represent the various resonant frequencies, while the line to the left of the shaded region represents terminal velocity.

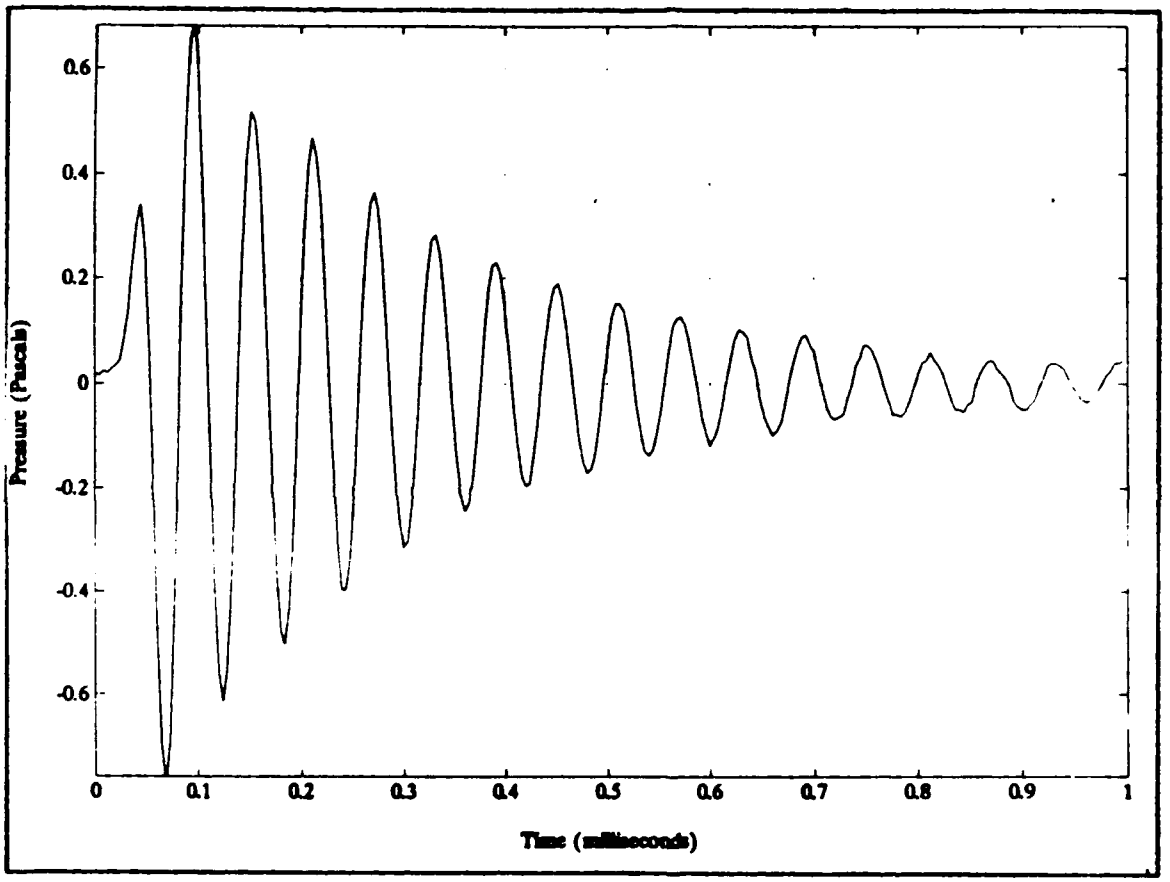

Figure 2. Acoustic pressure of a bubble in salt water produced by a 0.985 mm drop falling at terminal velocity perpendicular to the surface.

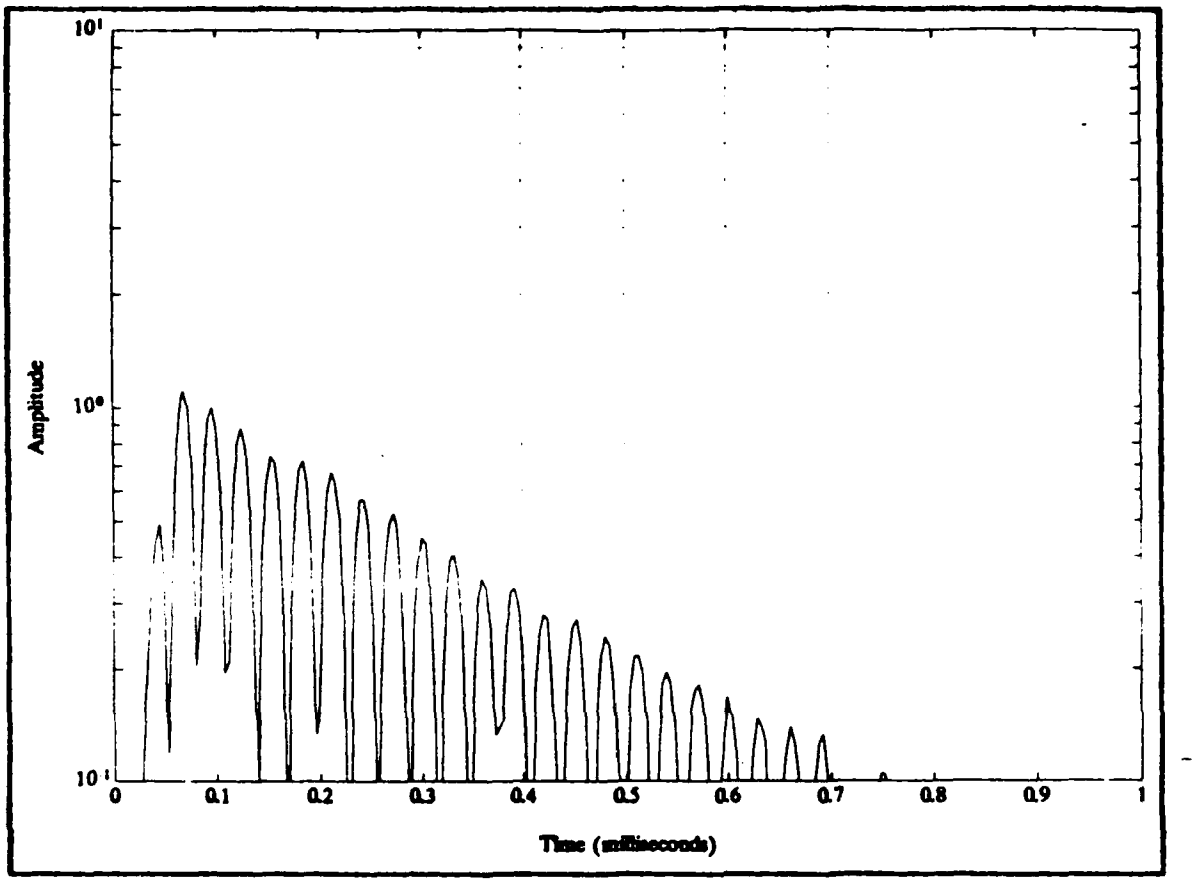

Figure 3. Semi-log plot of the rectified pressure of bubble in salt water: This is the same bubble as in Figure 2. The plot was normalized by dividing the entire signal by the highest absolute peak pressure.

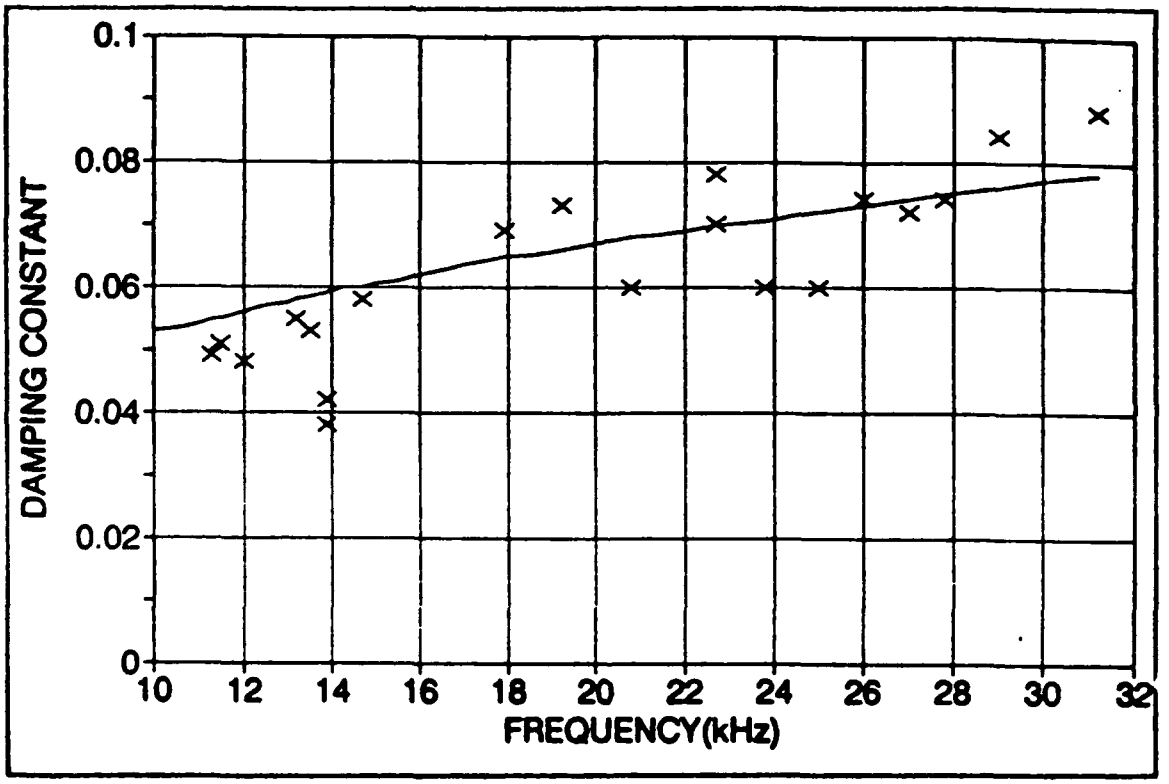

Figure 4. Experimental damping constants from Type 1 bubbles in fresh water (x) and theoretical damping constant for fresh water (line) versus frequency.

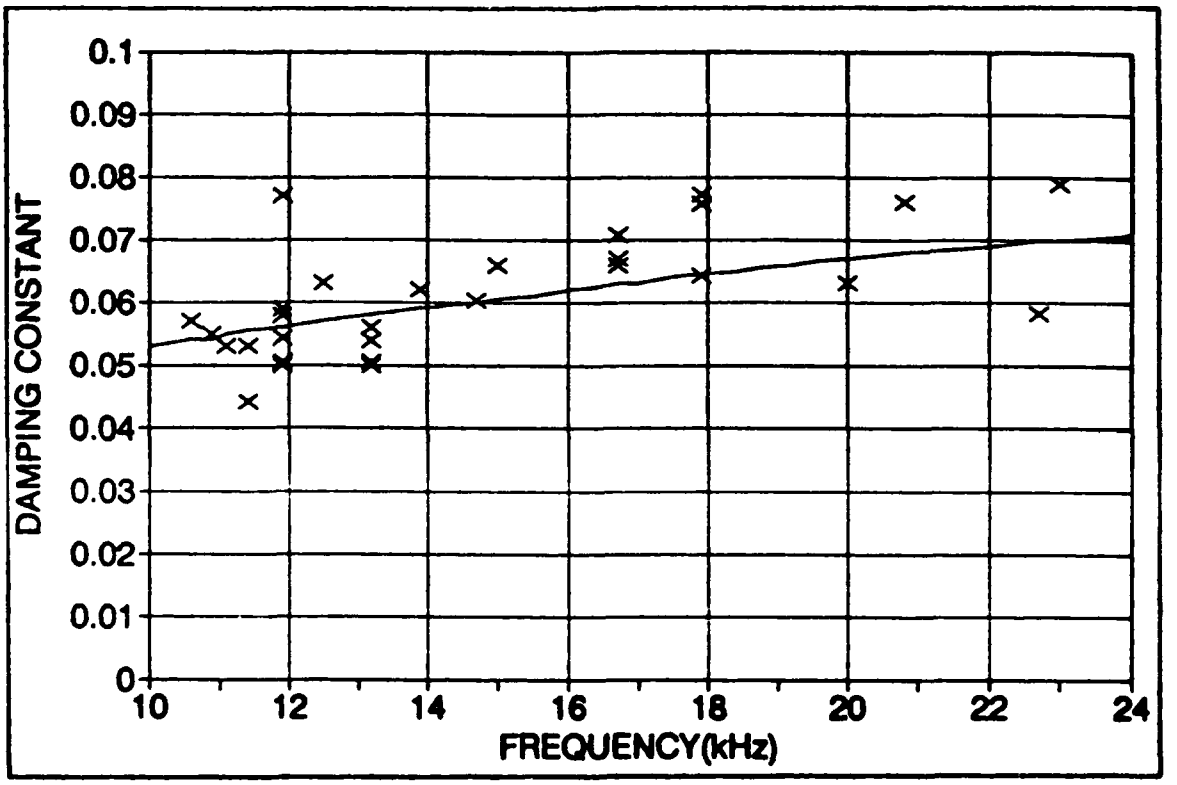

Figure 5. Experimental damping constants from Type I bubbles in salt water (x) and theoretical damping constant for fresh water (line) versus frequency.

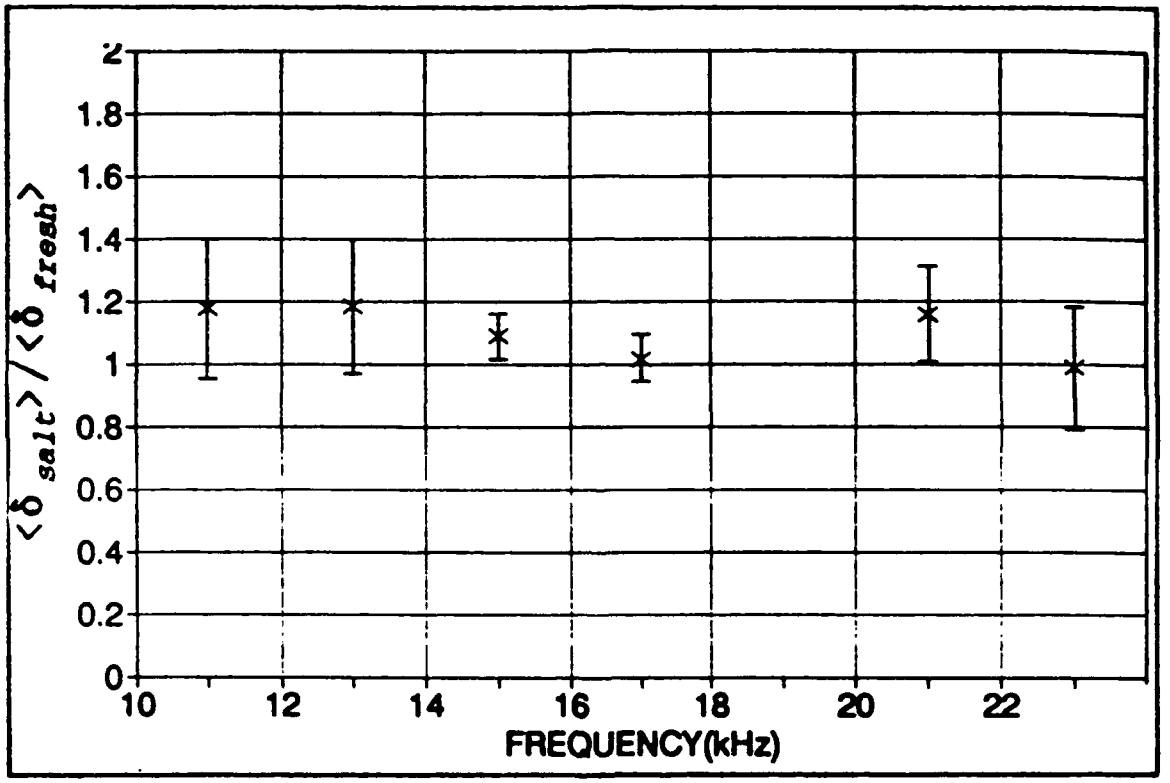

Figure 6. Ratio of average salt water δ to the average fresh water δ.

IV. DAMPING CONSTANT FOR FRESHWATER TEMPERATURE DIFFERENCES

A. EXPERIMENT

The data analyzed for this portion of the thesis were originally recorded by Jacobus (1991) during his studies of the dependance of sound radiation on temperature for large drops in fresh water. The drop size diameters used were 3.63 mm and 4.20 mm. All of the drops were produced by a standard medical intra-venous drip bag with a calibrated glass eye dropper attached to the end. This produced a stream of separated drops with an adjustable drop rate. The drip bag was placed at the top of a 3 m x 3 m x 26 m vertical utilities shaft, with sufficient height to ensure that the drops reached terminal velocity before impacting on the water surface. The temperature of the drops analyzed was varied between 11 and 40°C.

All the drops fell into the 1.5 m deep by 1.5 m diameter tank described in Chapter Three. The surface temperature of the water in the tank was changed from 21 to 27, 28 and 29°C. By comparing the temperature of the water in the tank with the varying temperature of the drops, it was possible to produce absolute drop-surface temperature differences of +6, -13, +17 and +19°C. The temperatures were all measured by Navy-issue

thermometers with an overall range of -20 to +50°C. The accuracy of the thermometers was ±0.5°C.

To record the sound produced by the bubbles, a hydrophone similar to an LC-5, but constructed in this lab, was used. It had a sensitivity of -91.5 dB re 1V per Pa with a frequency response flat to at least 200 kHz. It was placed at a depth of 6.0 cm. The output of the hydrophone was amplified by a PAR 113 Low Noise Pre-Amplifier with a gain of 2000. The signal was then fed into a Krohn-Hite band pass filter passing frequencies between 1 and 30 kHz.

Because these bubbles usually oscillated at a lower frequency (2-10 kHz) compared to the smaller bubbles (15±5 kHz) of the previous chapter, many of the signals were not "clean" due to interference from the combined affects of longer wavelengths (0.37 meters at 4 kHz) and a small tank radius (0.75 meters). The interference made it impossible to accurately fit a line on the semi-log plot of the bubble oscillation, calculate the slope and determine t_o. As a result "unclean" signals were discarded, leaving only 19 signals (over 40 signals were discarded) to be evaluated. All the data was analyzed in the same manner as described in Chapter Three.

B. RESULTS

Figure 7 shows the theoretical damping constant for fresh water (Devin, 1959) and the experimental damping constants (+ represents $\Delta T=6^{\circ}C$, * represents $\Delta T=13^{\circ}C$, x represents $\Delta T=17^{\circ}C$ and I represents $\Delta T=19^{\circ}C$). The experimental results for each absolute temperature difference were separated, based on their frequencies, into bins 1 kHz wide and averaged. The ratio of these averages to the theoretical damping constant for the midpoint of the frequency band are taken as shown in Table 1.

TABLE 1. RATIO OF AVERAGE EXPERIMENTAL TO THEORETICAL DAMPING CONSTANT

FREQUENCY	$\delta_{\Delta T=6}/\delta_{TH}$	$\delta_{\Delta T=13}/\delta_{TH}$	$\delta_{\Delta T=17}/\delta_{TH}$	$\delta_{\Delta T=19}/\delta_{TH}$
2-3 kHz	0.87	0.79	0.82	0.89
3-4 kHz	0.80	-	-	1.27
4-5 kHz	0.83	-	-	-
5-6 kHz	-	-	1.02	-
7-8 kHz	-	0.78	-	-
8-9 kHz	-	-	1.22	-
9-10 kHz	-	0.88	-	-
Average	0.83±0.04	0.82±0.06	1.02±0.20	1.08±0.27

There is limited evidence of an increase in δ as a function of increase in absolute temperature difference in Figure 7. Figure 8 shows the dependence on absolute temperature difference of the mean ratio of the experimental and theoretical damping constants (the last row of Table 1).

For each data point in Figure 8, every data point in Figure 7 with the same absolute temperature difference was divided by the theoretical damping constant with the same resonance frequency, added and averaged. From an absolute temperature difference of 6°C to an absolute temperature difference of 19°C there is an increase in the average ratios of the experimental to theoretical damping constant from 0.83±0.04 to 1.08±0.27. Since the acoustic energy is inversely proportional to $1/\delta$ as shown by (19) these results suggest that as the absolute temperature difference increases, the energy from a bubble may decrease because of the greater damping. However, the large standard deviation found on the average ratios for absolute temperature differences of 17 and 19°C as well as the fact that the average ratio increases from 0.82±0.06 to 1.02±0.20 over a change in absolute temperature difference of only 4°C (ΔT=13°C to ΔT=17°C) when it is relatively consistent over a change in absolute temperature difference of 7°C (ΔT=6°C to ΔT=13°C) suggests that the change in absolute temperature difference may not be statistically significant. Therefore, based on Figure 8, the conclusion of this analysis is that the absolute temperature difference between the drop and water surface has little affect on the damping constant.

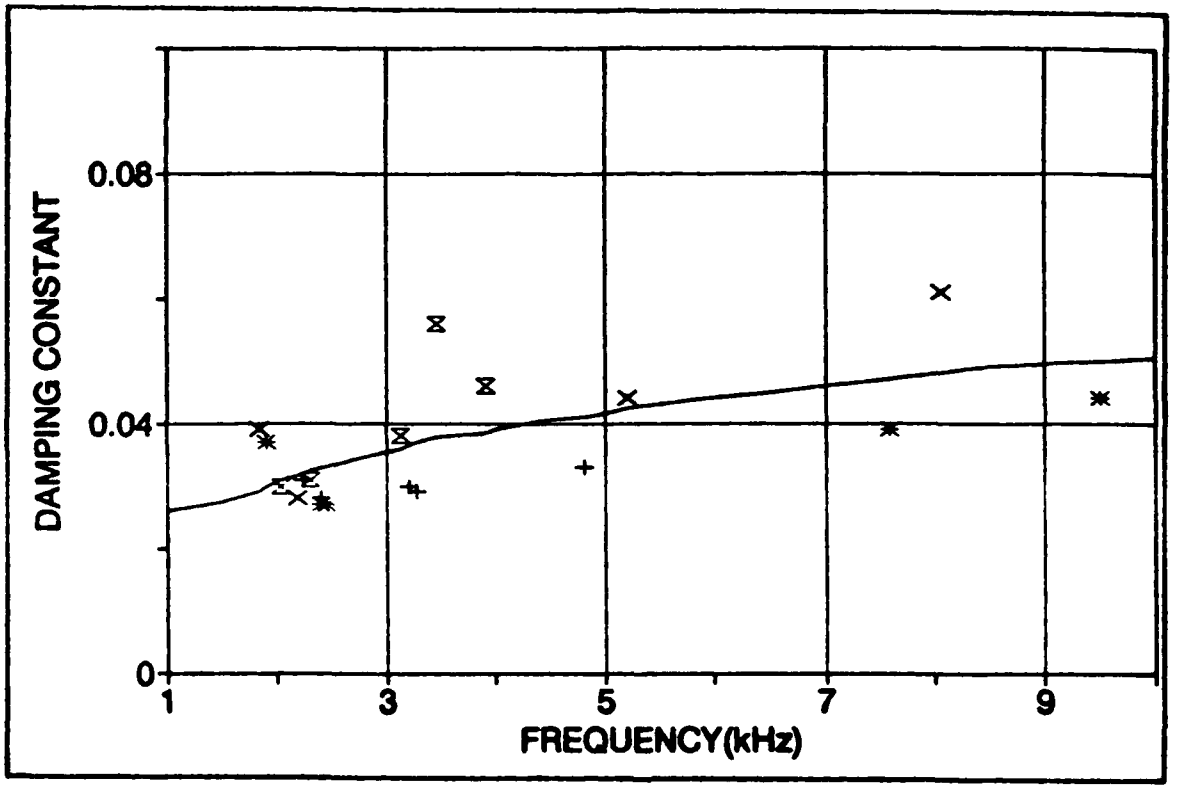

Figure 7. Experimental damping constants at various absolute temperature differences (+ represents ΔT=6°C, * represents ΔT=13°C, x represents ΔT=17°C and I represents ΔT=19°C) and theoretical damping constant (line) versus frequency.

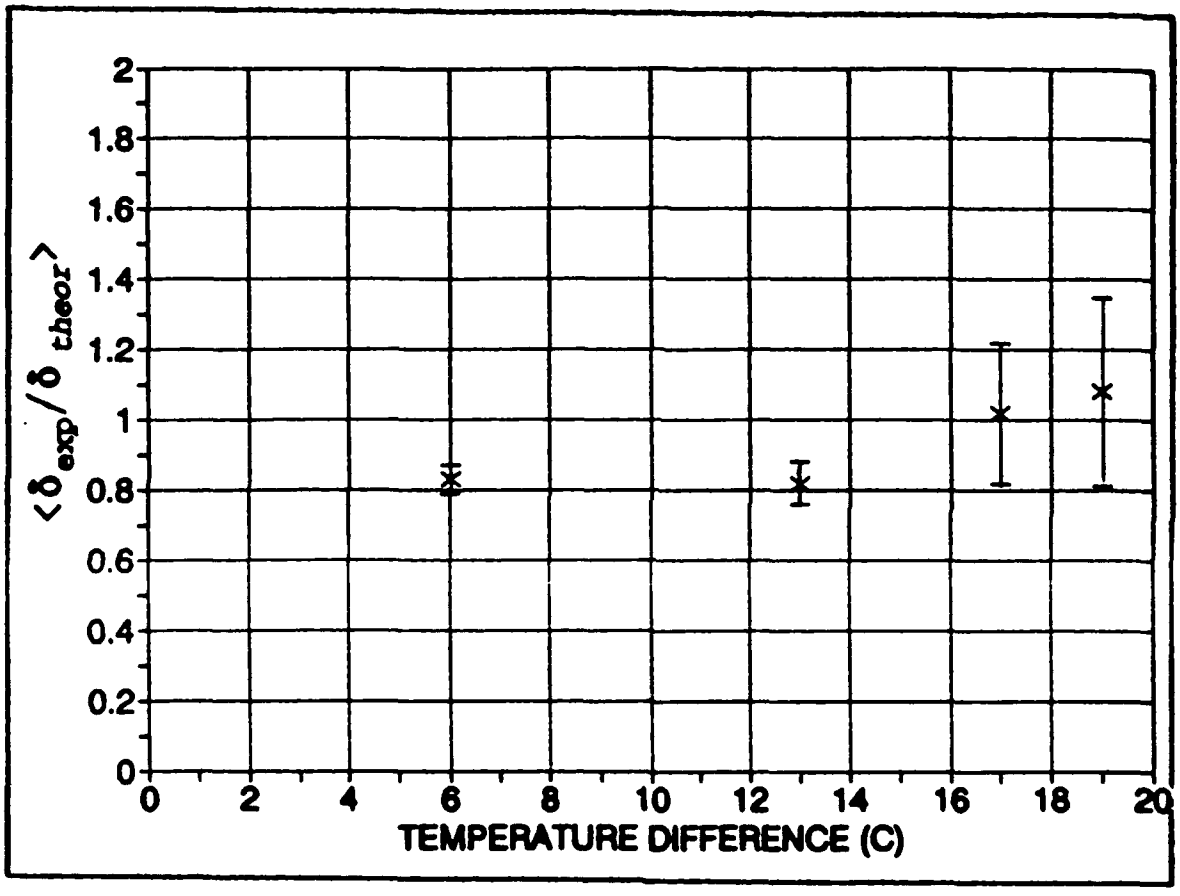

Figure 8. Ratio of average experimental damping constant to theoretical fresh water damping constant versus temperature difference.

V. EFFECT OF SALINITY ON PEAK PRESSURE

A. EXPERIMENT

The data analyzed here were the bubbles with resonance frequencies ranging 10-16 kHz (resonance frequency range for bubbles produced by 0.985 mm drops falling a terminal velocity in accordance with Figure 1) created by 0.985 mm raindrops described in Chapter Three. In this analysis, the highest absolute peak pressure was the only portion of each signal used and consequently many signals which were not used during the damping constant analysis (because of interference effects) were used here. For each bubble, the recorded signal was converted to pressure at the hydrophone in pascals (Pa), using the following equation (Ostwald,1992)

$$p_{byd} = \frac{V}{G\,M} \qquad (21)$$

where V is the voltage recorded by computerscope, G is the amplifier gain and M is the hydrophone sensitivity (V/Pa). The hydrophone response was assumed to be omnidirectional. To convert this to equivalent pressure at one meter on axis, p_{byd} was multiplied by the near field correction and a correction

which accounted for the dipole radiation pattern (Ostwald, pp 64-65,1992).

B. RESULTS

A total of fifty bubbles created by 0.985 mm raindrops (25 salt and 25 fresh water) were analyzed to determine the effects of salinity on the axial peak pressure at one meter. The peak pressures used in analyzing the bubbles were obtained two different ways and the results compared. The initial method was to use the highest absolute peak pressure of the entire oscillation while the second method was to use the average of the absolute values of the highest adjacent positive and negative peak pressures. The peak pressures obtained from these methods are plotted versus frequency in Figure 9 (using highest absolute peak pressure) and Figure 10 (using average of adjacent positive and negative peaks). In both figures, there appears to be a trend of the fresh water values (+) and salt water values (x) slightly increasing with frequency as would be expected in accordance with (16) if the dipole strength were constant.

However there is no reason to assume that the dipole strength remains constant. To obtain the Figures 11, 12, 13, 14, 15 and 16, the fresh and salt water pressures from Figures 9 and 10 were separated into 1 kHz frequency bands (10-11, 11-

12, 12-13, 13-14, 14-15, and 15-16 kHz) added up and the mean pressure calculated for each bin. To eliminate any frequency effect, these mean fresh and salt water peak pressures were then divided by the square of the middle frequency of the bin (f^2), since equation (16) shows that P_d/f^2 is a function only of D with all the other factors being constants. Figure 11 (using highest absolute peak pressure) and Figure 12 (using average peak) show that for fresh water P_d/f^2, and therefore the dipole strength, may decrease slightly with frequency. In salt water Figure 13 (using highest absolute peak pressure) and Figure 14 (using average peak) show that P_d/f^2 may decrease with frequency more rapidly in salt water than in fresh water. Figures 15 and 16 take the ratio of P_d/f^2 for fresh water to P_d/f^2 for salt water for the highest absolute peak and average peak cases respectively. The figures show that the average values of P_d/f^2 are usually greater in fresh water than salt water. Despite the low statistical confidence of several points (indicated by large error bars), both figures suggest a trend of increasing dipole strength ratio with frequency.

Since, in accordance with (16), the dipole pressure is proportional to the dipole strength, the average P_d over a wide range of frequencies is apparently less in salt water than in fresh water. Summing all of the absolute peak pressures used in this experiment and calculating the fresh

and salt water means produced values of 0.35±.09 Pa for salt water and 0.39±.10 for fresh water. Doing the same for the average adjacent positive and negative peak pressures produced mean pressures of 0.32±.07 for salt water and 0.36±.05 for fresh water. All four of these values are consistent with the average peak pressure of a bubble produced by 0.985 drop calculated by Kurgan (1989), shown in Figure 17. In summary it appears the average peak pressure of a bubble in salt water is slightly less than that of a comparable bubble in freshwater. This ratio may be frequency dependent.

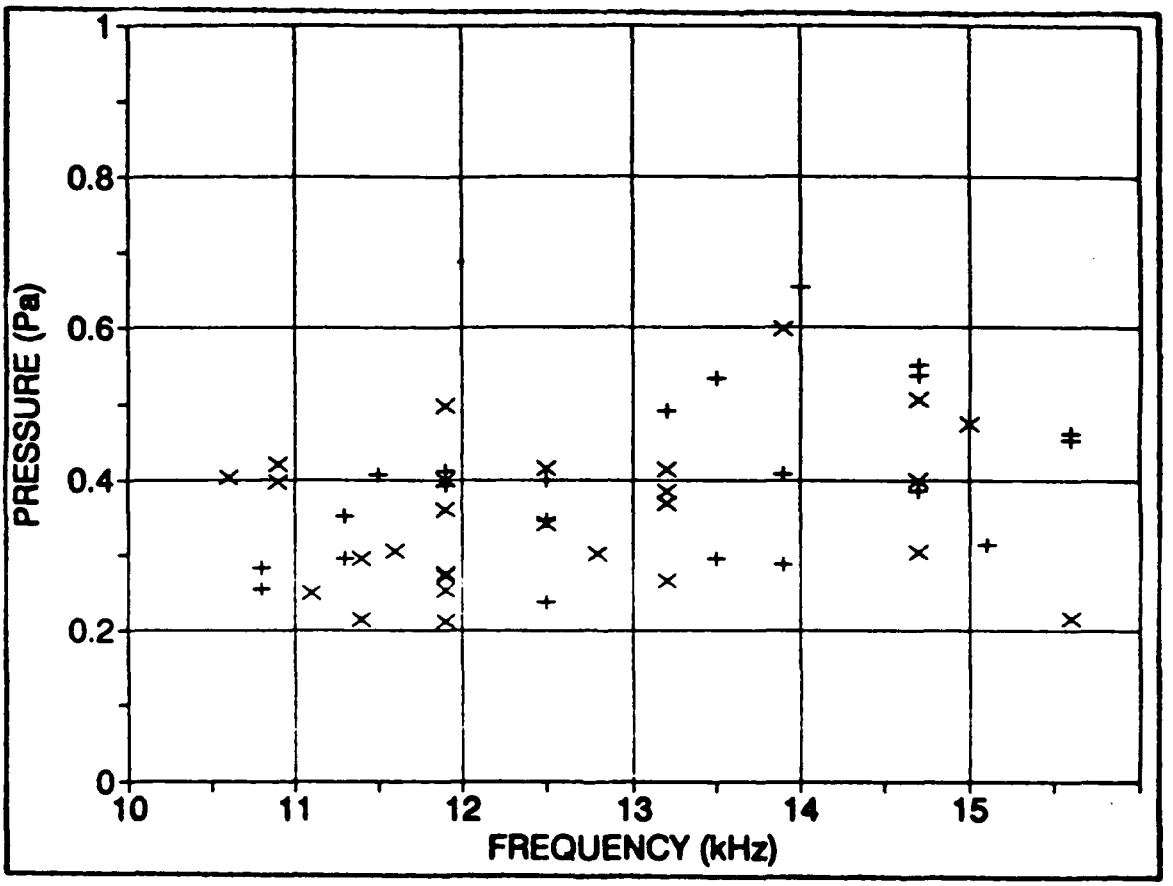

Figure 9. Absolute peak pressures obtained from bubbles produced by 0.985 mm raindrops landing on fresh water (+) and salt water (x) versus frequency.

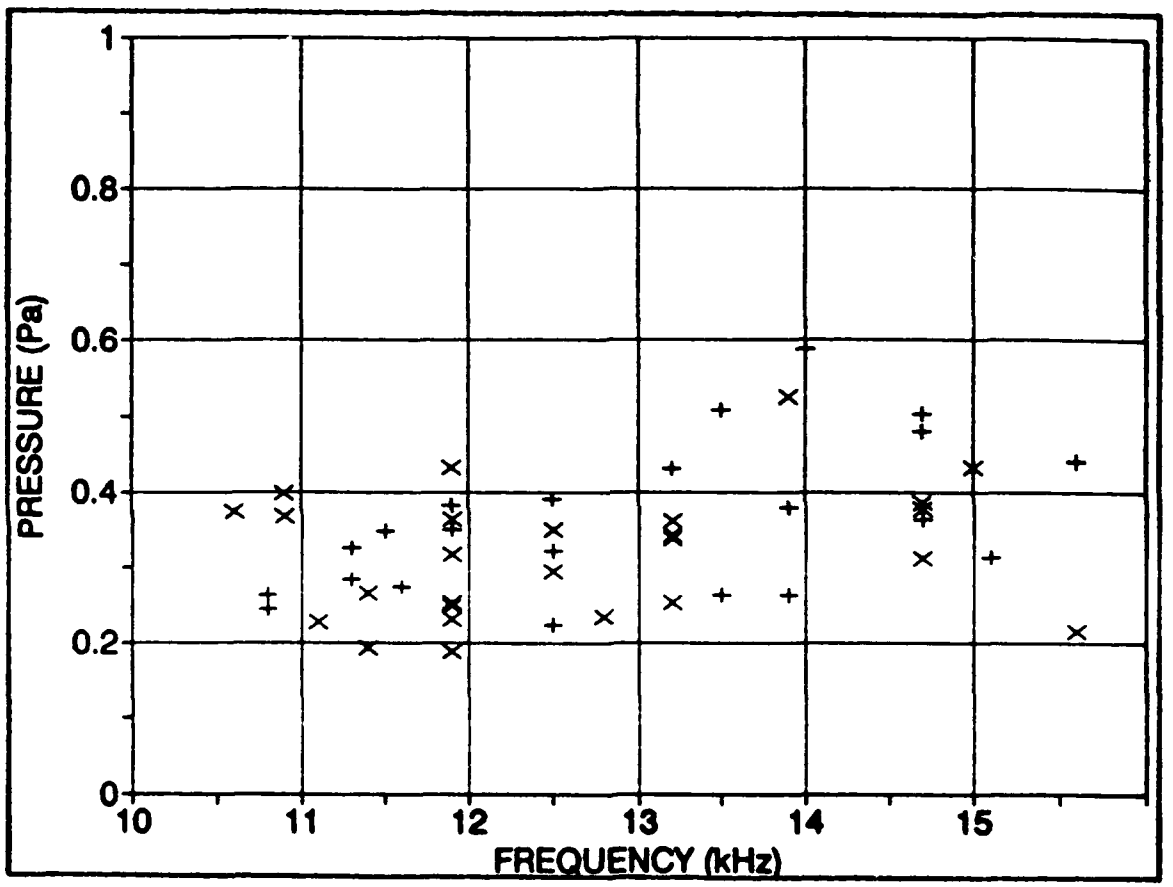

Figure 10. Pressures which are the average of adjacent positive and negative peak pressures obtained from bubbles produced by 0.985 mm raindrops landing on fresh water (+) and salt water (x) versus frequency.

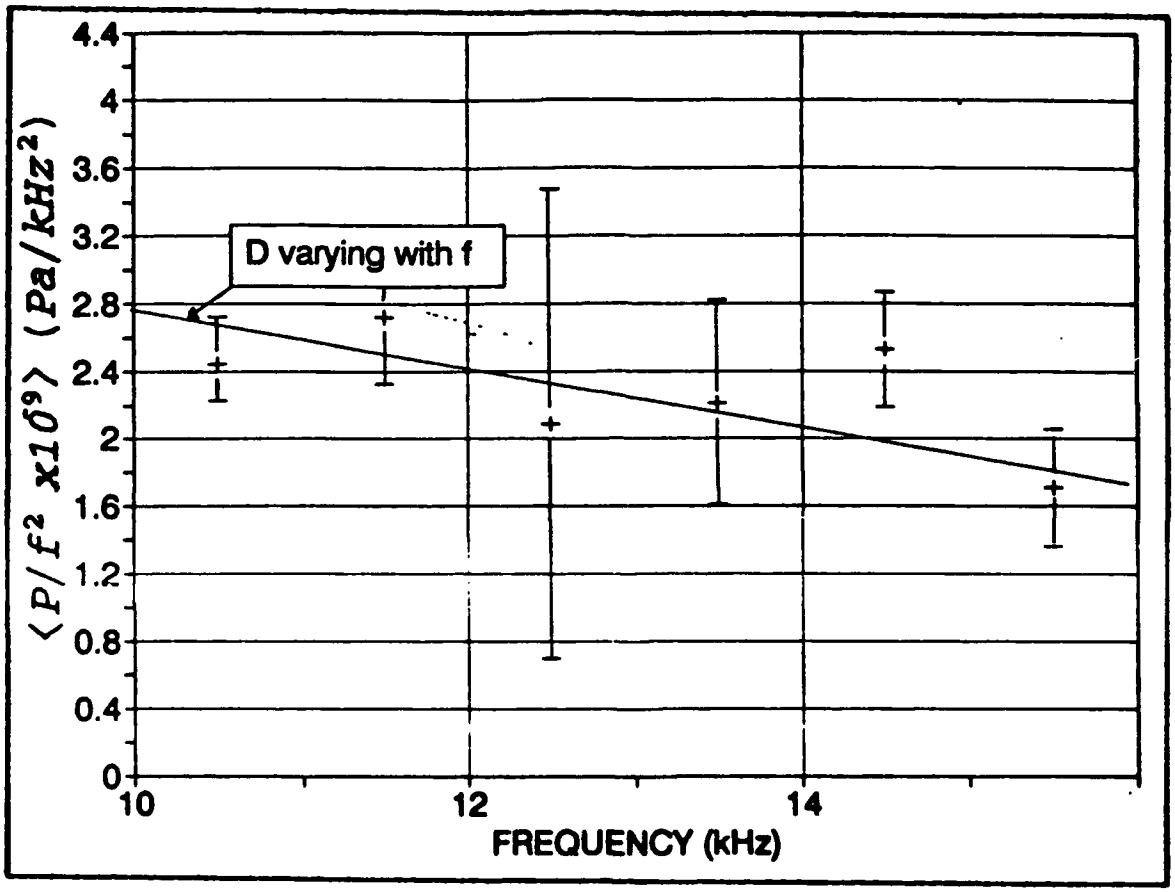

Figure 11. Average P_a/f^2 for the peak pressure of bubbles produced by 0.985 mm drops falling on fresh water versus frequency.

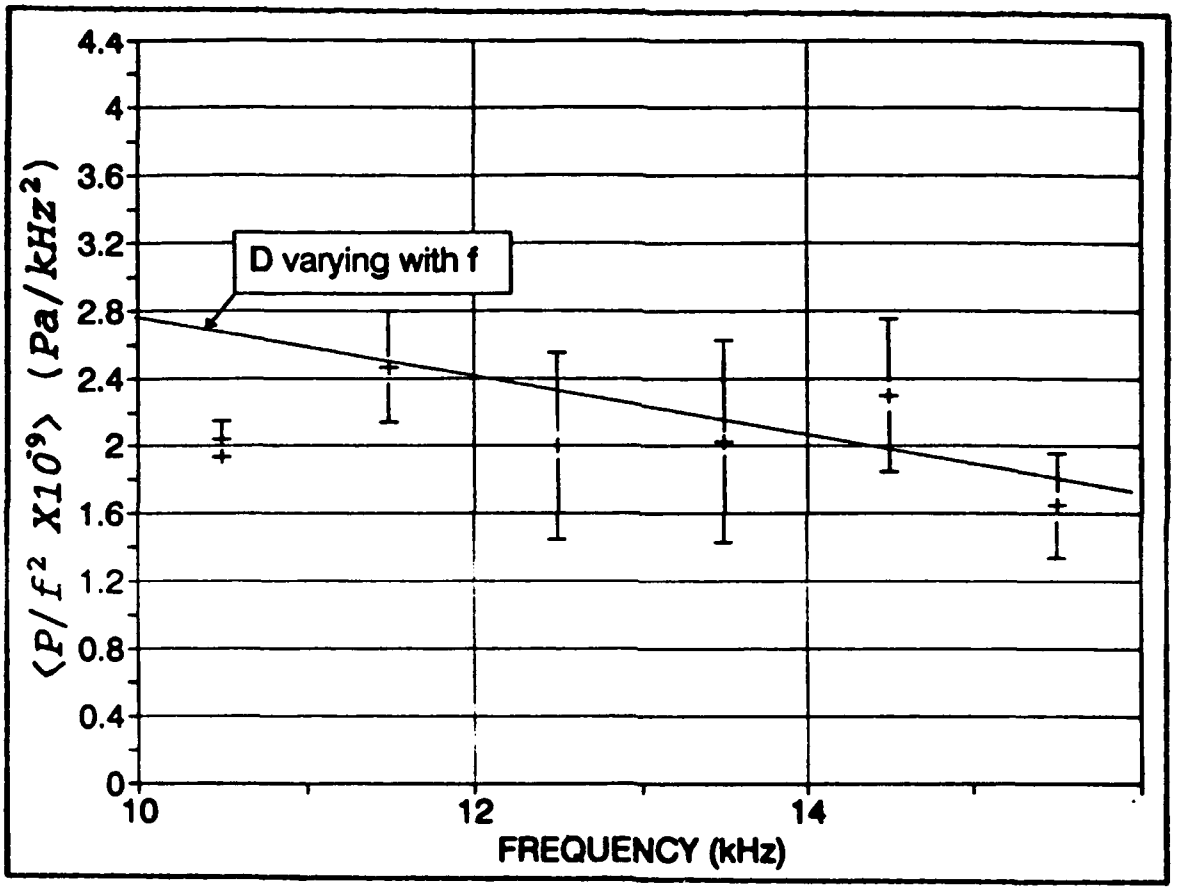

Figure 12. Average P_d/f^2 for pressures which are the average of adjacent positive and negative peak pressure of bubbles produced by 0.985 mm drops falling on fresh water versus frequency.

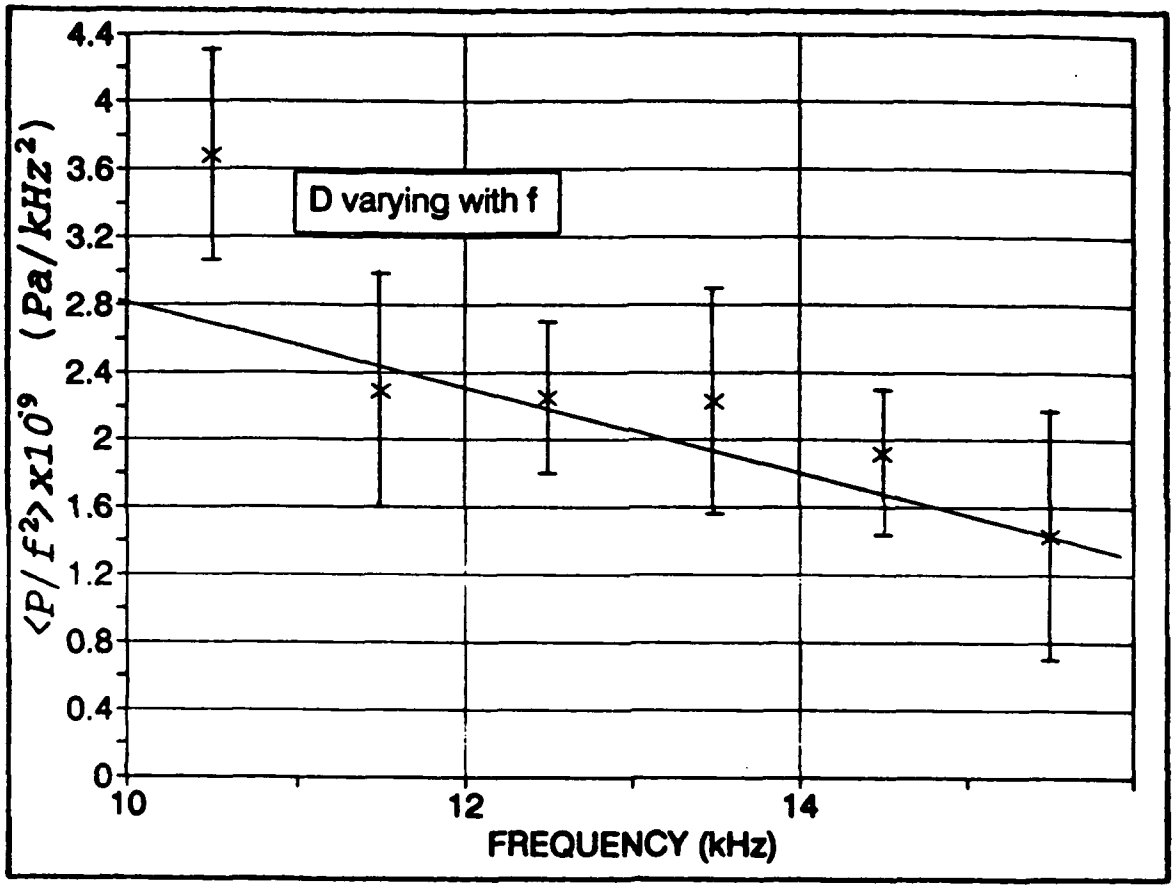

Figure 13. Average P_d/f^2 for the peak pressure of bubbles produced by 0.985 mm drops falling on salt water versus frequency.

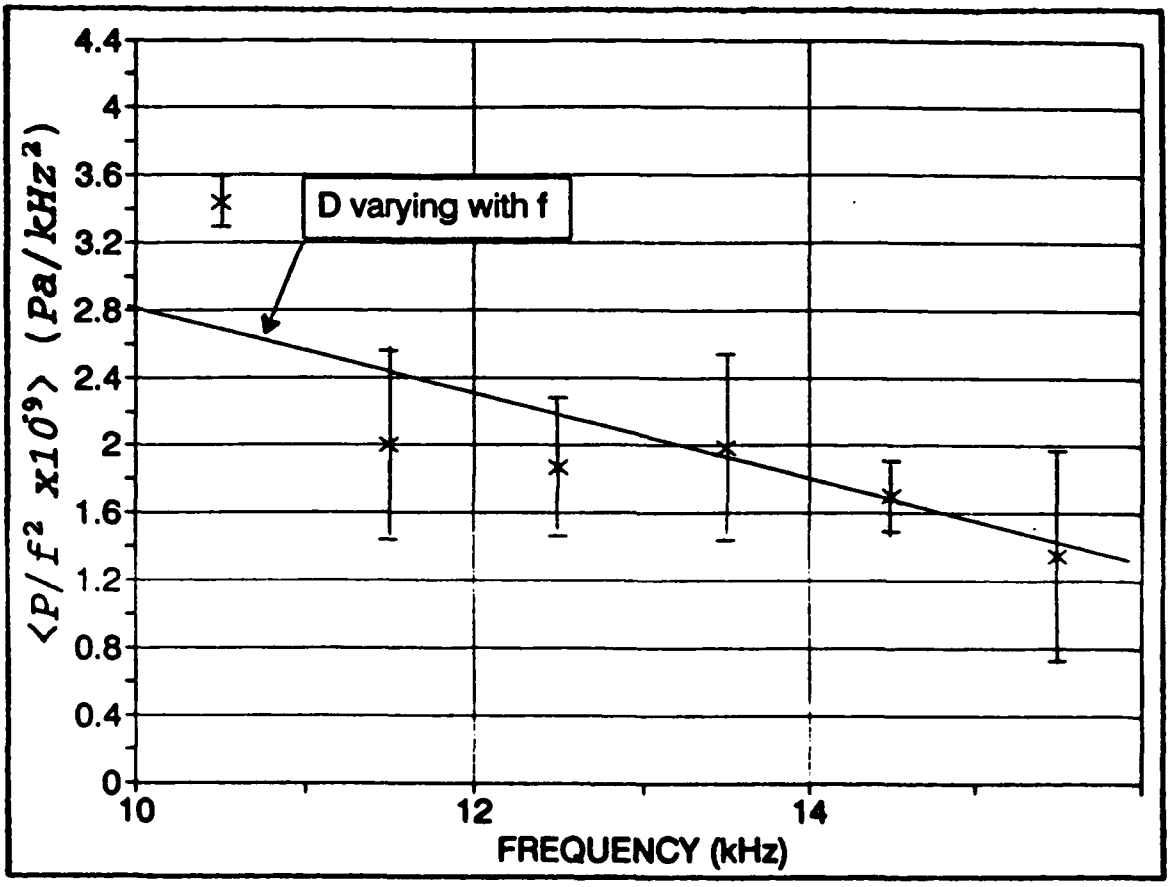

Figure 14. Average P_d/f^2 for pressures which are the average of adjacent positive and negative peak pressure of bubbles produced by 0.985 mm drops falling on salt water versus frequency.

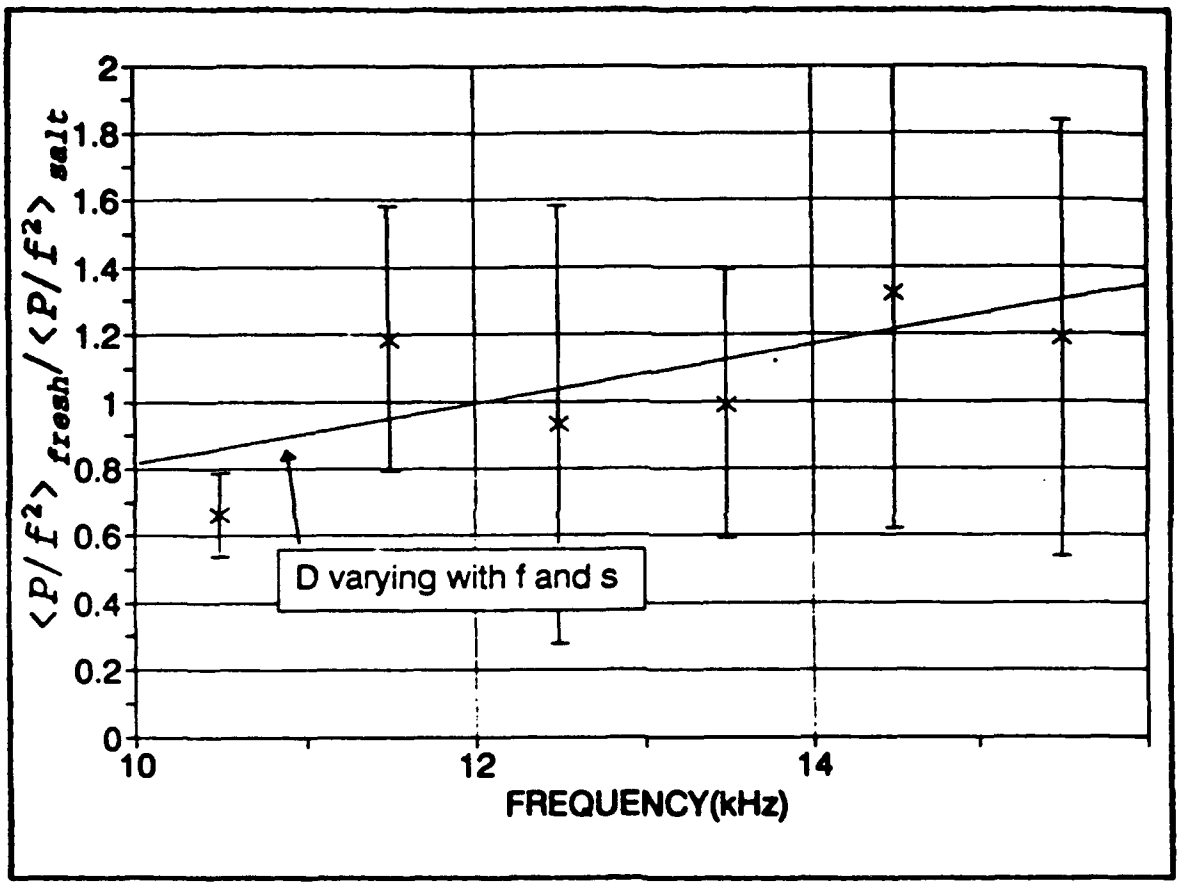

Figure 15. Ratio of fresh water P_d/f^2 to salt water P_d/f^2 versus frequency. Pressures are the peak pressures of bubbles produced by 0.985 mm raindrops.

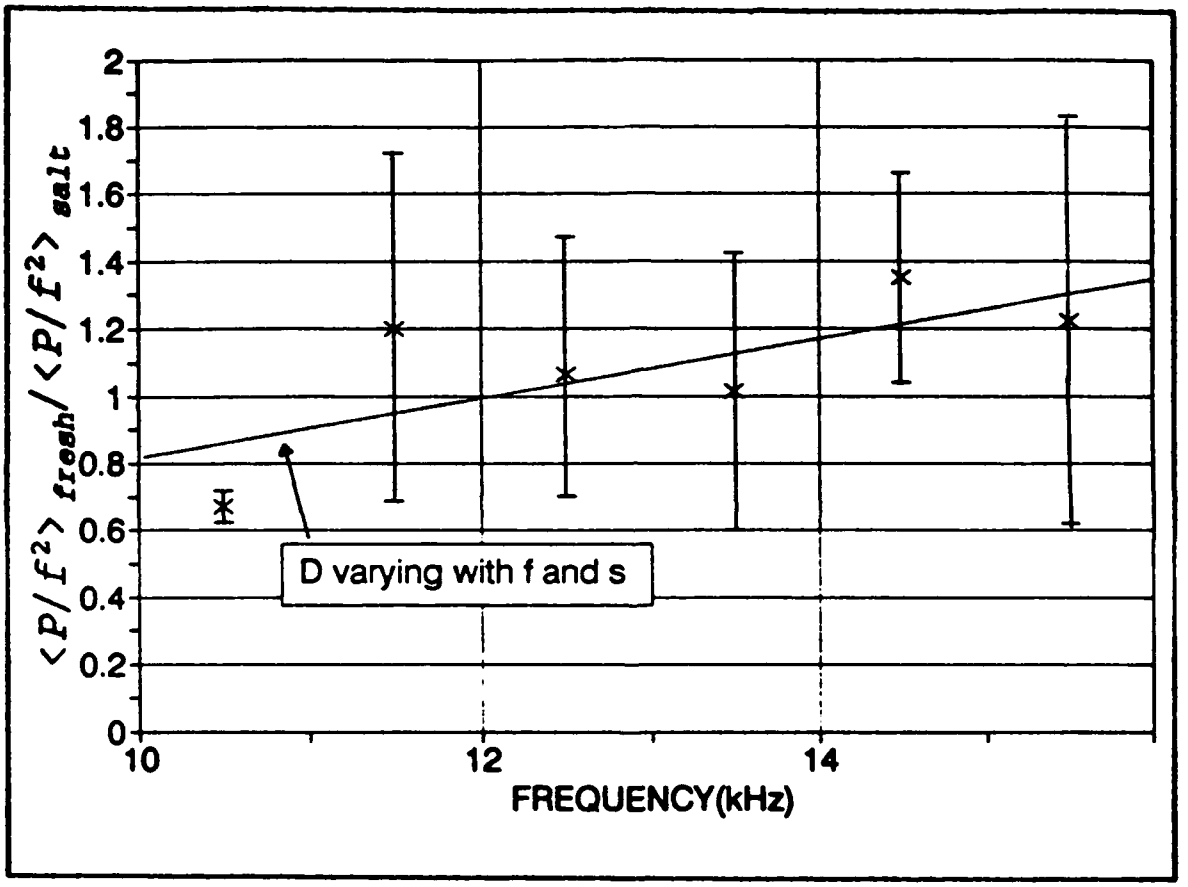

Figure 16. Ratio of fresh water P_d/f^2 to salt water P_d/f^2 versus frequency. Pressures are the average of adjacent positive and negative peak pressures of bubbles produced by 0.985 mm raindrops.

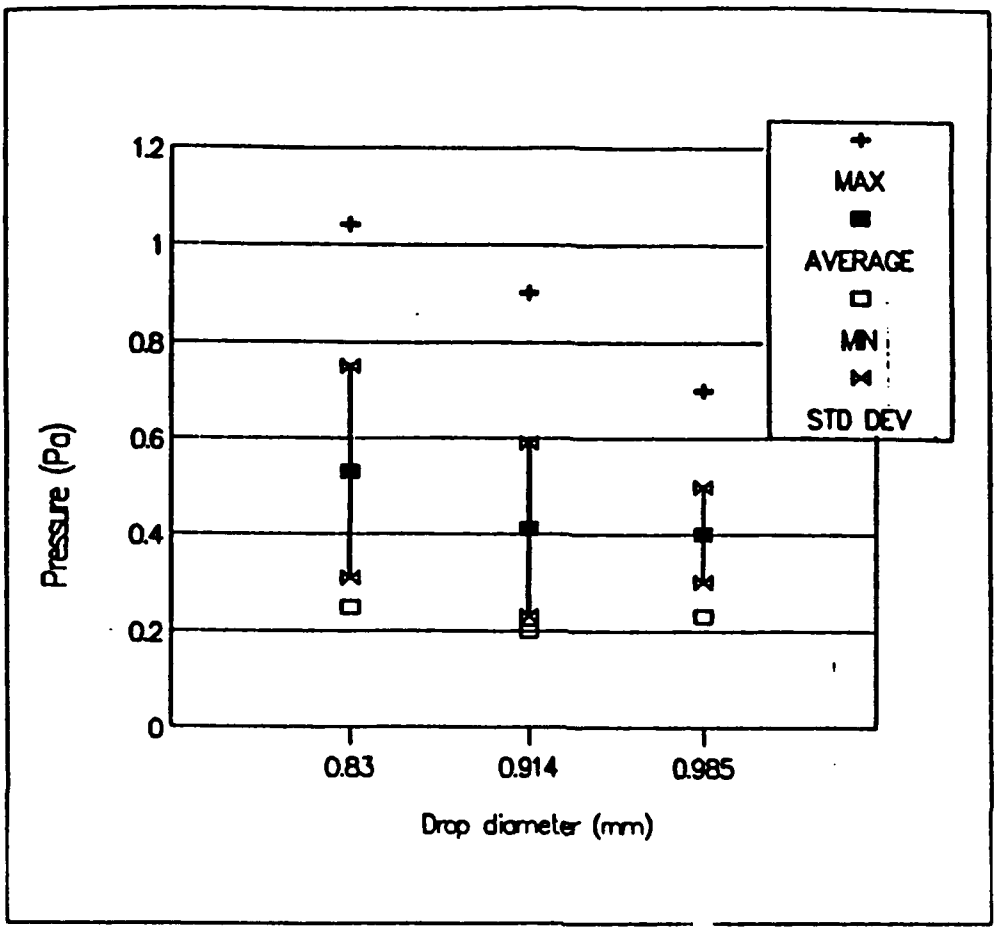

Figure 17. Average peak axial pressures for bubbles. From Kurgan (1989).

VI. TEMPERATURE EFFECTS ON PEAK PRESSURE

A. EXPERIMENT

The data analyzed here were the same as described in Chapter Four. Just as in the analysis of the effect of salinity on peak pressure, the highest absolute peak pressure for each bubble was analyzed. Once again, many signals which were not used during the damping constant analysis (because of showing interference effects) were used in this analysis. The data was processed in the manner described in Chapter Five to determine pressure on axis at 1 meter (m) from the source in pascals.

B. RESULTS

To determine the effects of temperature difference on the peak pressure 55 bubbles created by 4.2 mm raindrops were studied (18 with a 6°C temperature difference between the drop and water surface, 19 with 13°C temperature difference and 18 with a 19°C temperature difference). Initially the axial (1 meter) peak pressures of these bubbles are computed in pascals and plotted versus frequency as shown in Figure 18. As in Figures 9 and 10, the experimental values for peak pressure

increases with frequency as would be expected from (16). These values were divided by the square of there resonance frequency which produced a quantity with only one unknown, the dipole strength as shown by (16). The experimental values of P_d/f^2 are plotted versus frequency in Figure 19 where it can be seen, as was the case in Figures 11 and 12 in Chapter 5, that P_d/f^2 appears to slightly decrease with frequency in fresh water. Summing up all the experimental values of P_d/f^2 for each absolute temperature difference and calculating a mean P_d/f^2 for each absolute temperature difference produced Figure 20. Figure 20 shows that P_d/f^2 and therefore the dipole strength increasing with the absolute temperature difference between the drop and the surface.

Thus, in summary, as the absolute temperature difference between the raindrop and water surface increases so does the dipole strength. This dipole strength, in turn, increases the peak pressure as would be expected from (16).

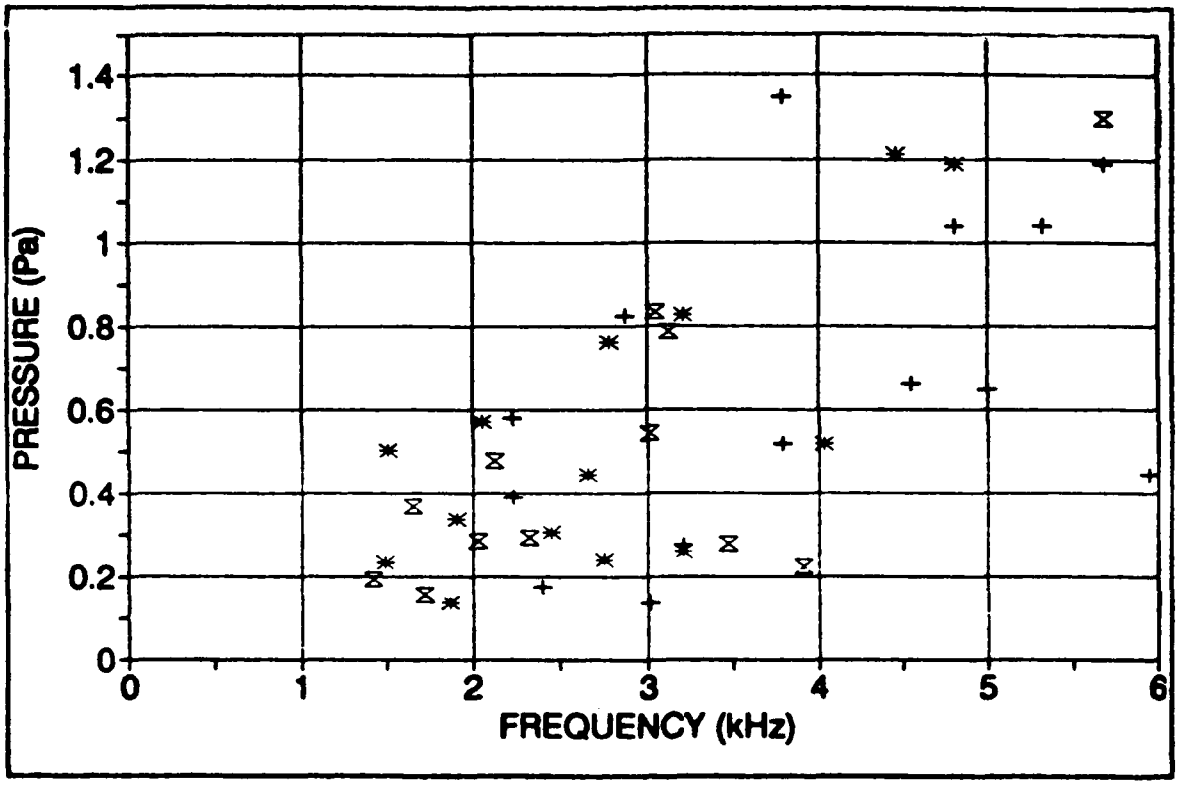

Figure 18. Peak pressures for bubbles produced by 4.2 mm raindrops with various temperature differences between the drop and water surface. The + represents $\Delta T=6^{\circ}C$, * represents $\Delta T=13^{\circ}C$ and X represents $\Delta T=19^{\circ}C$.

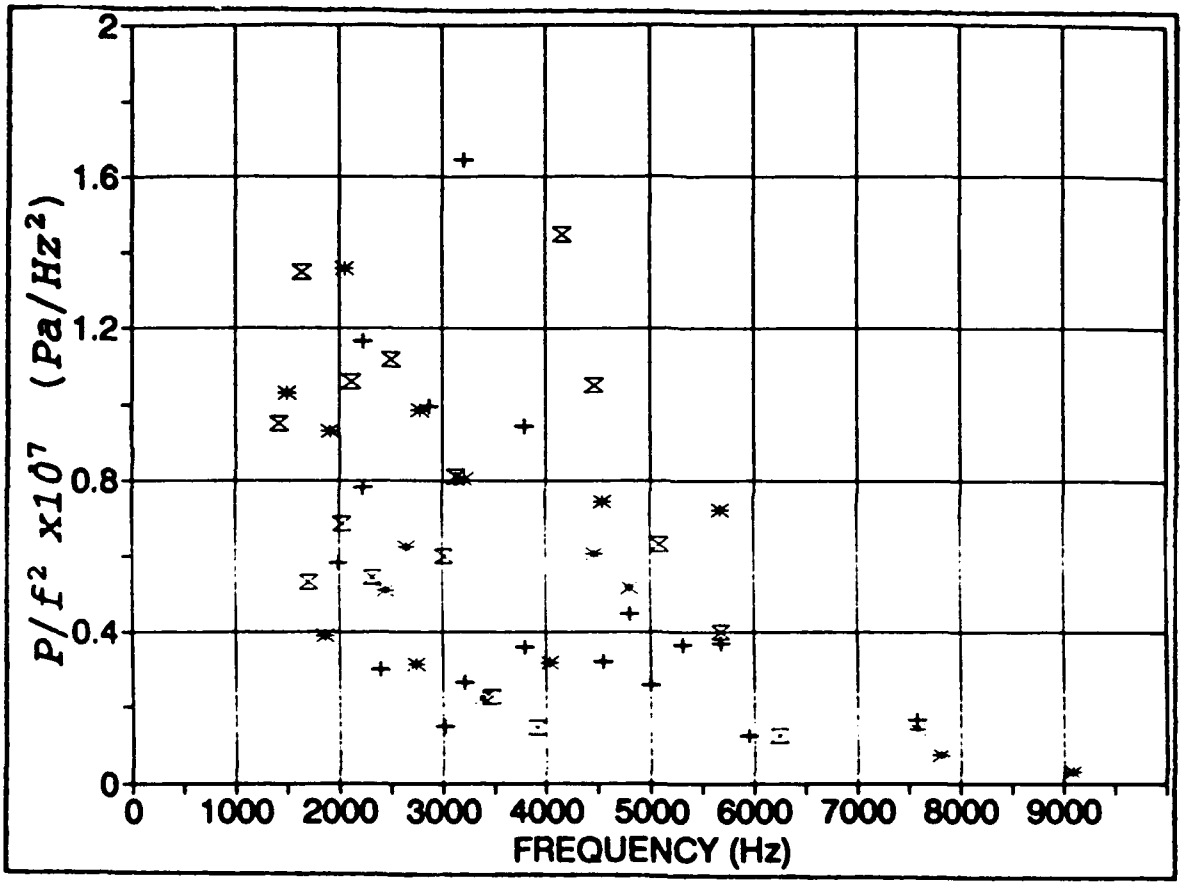

Figure 19. P_d/f^2 for bubbles produced by 4.2 mm raindrops with various temperature differences between the drop and water surface. The + represents $\Delta T=6^{\circ}C$, * represents $\Delta T=13^{\circ}C$ and X represents $\Delta T=19^{\circ}C$.

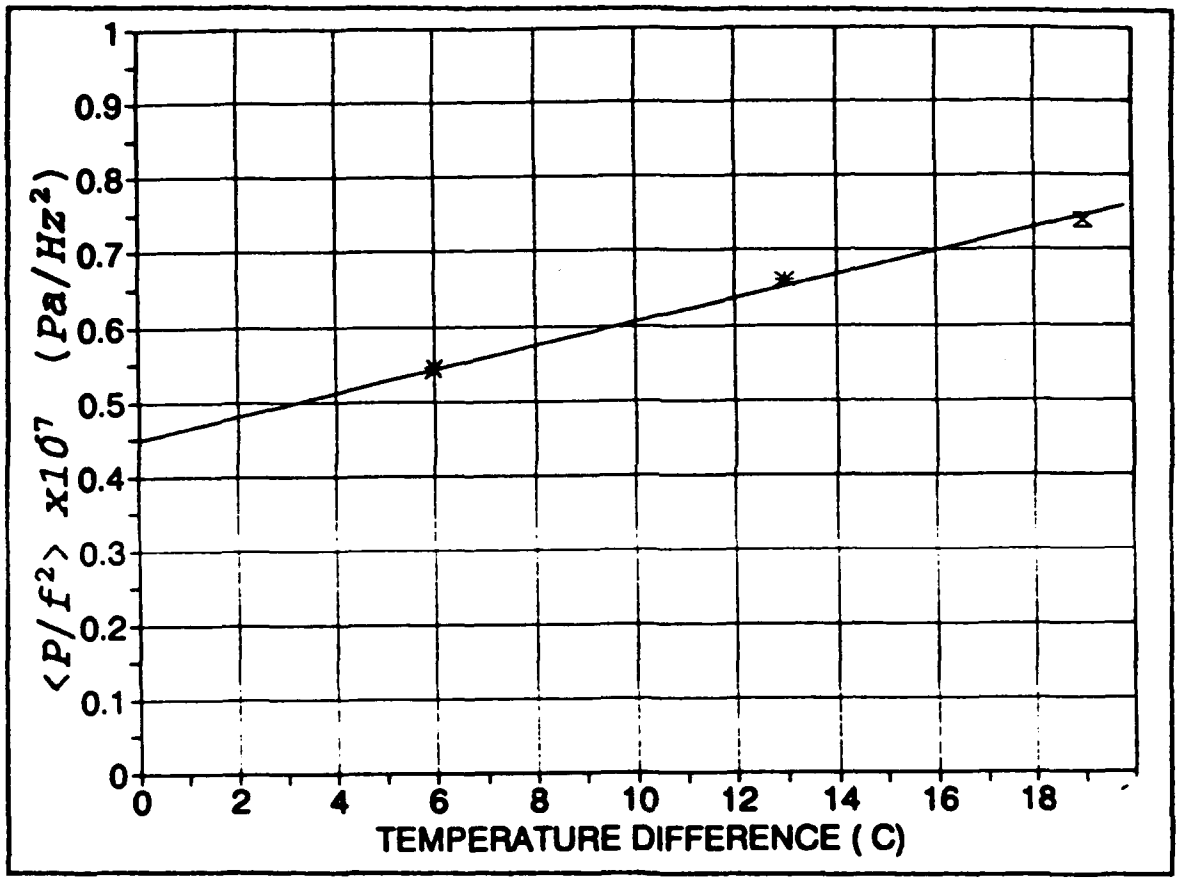

Figure 20. Average P_d/f^2 versus temperature difference for bubbles produced by 4.2 mm raindrops.

VII. BUBBLE ENERGY

Combining the data produced from the analysis performed in Chapters Three through Six with (19) makes it possible to determine the affect of salinity and temperature on the actual energy produced by a spherical bubble oscillating in water.

A. SALINITY

The data from Chapters Three and Five can be used with (18) to compute the energy produced by bubbles created from 0.985 mm drops striking fresh and salt water. The data were then separated into 1 kHz bins, the mean fresh and salt water energy computed, and the ratio of the fresh to salt water energies determined for each bin. Figure 21 (using highest absolute peak pressure) and Figure 22 (using average of adjacent positive and negative peak pressures) show that the energy produced by a spherical bubble oscillating in freshwater is consistently greater than that of a bubble oscillating at the same frequency in salt water. Combining all data, the mean the energy produced by a bubble in freshwater is between 1.46±0.37 (using highest peak) and 1.59±0.32 (using average peak) times greater than the energy produced by a comparable bubble in salt water. This

corresponds to the results obtained by Jacobus (1991) for large raindrops.

B. TEMPERATURE

The data from Chapter Six (Figures 18 and 20) were used with (18) in an attempt to determine how the absolute temperature difference between the drop and surface affects the energy produced by the bubble. These results are plotted in Figure 23 which shows the average values of $P_d^2/f\delta$ (other variables in (18) are the same for every bubble and therefore do not affect the outcome) for the various absolute temperature differences. Figure 23 shows that the values for the energy produced by bubbles which result from 4.2 mm raindrops increases as the absolute temperature difference between the raindrop and water surface increases. This result is, once again, in agreement with Jacobus (1991).

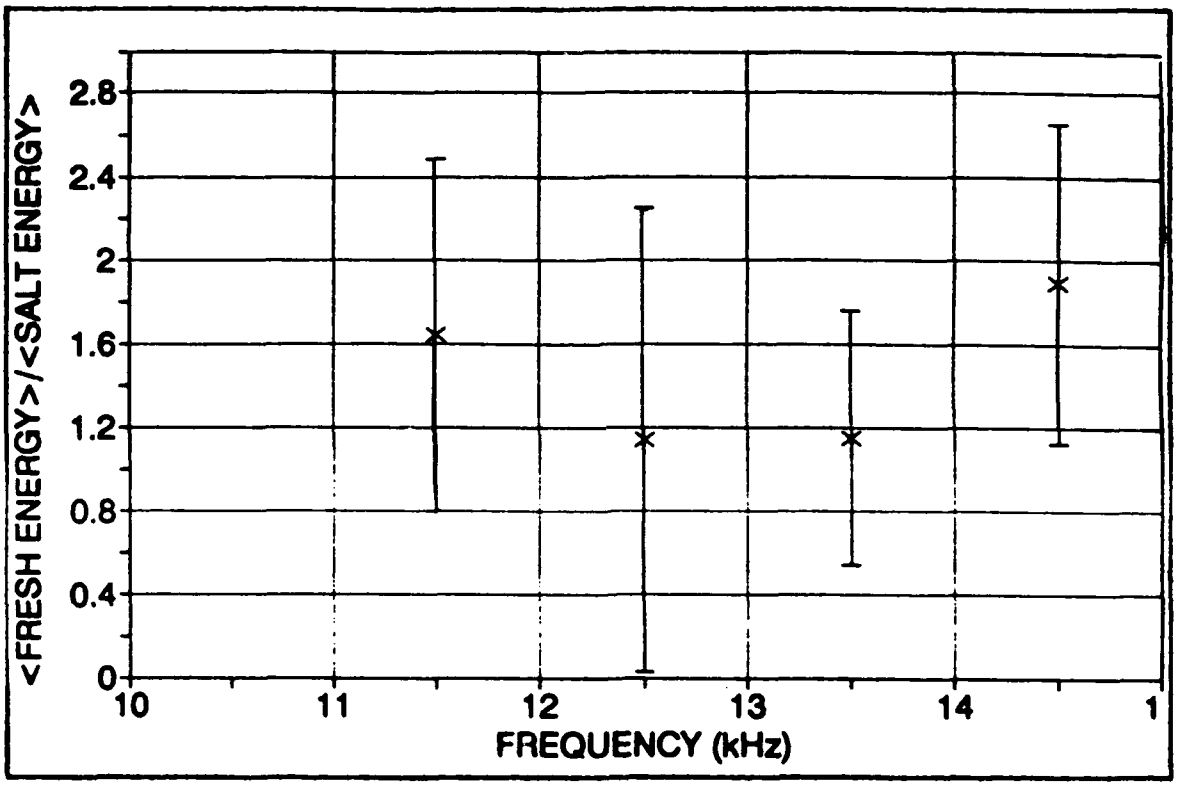

Figure 21. Ratio of the sound energy produced by bubbles resulting from 0.985 mm raindrops in fresh water to comparable bubbles in salt water. The pressures used for this figure were the absolute peak pressures.

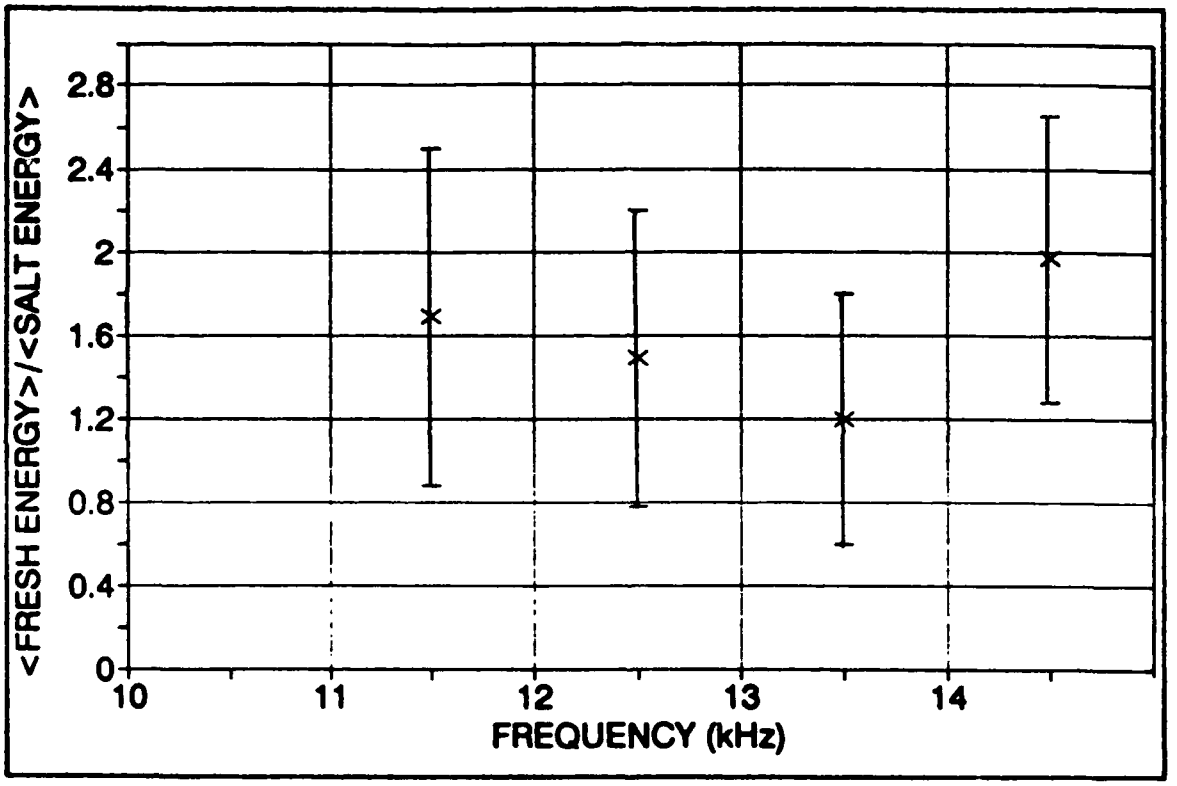

Figure 22. Ratio of the sound energy produced by bubbles resulting from 0.985 mm raindrops in fresh water to comparable bubbles in salt water. The pressures used for this figure was the average of the adjacent positive and negative peak pressures.

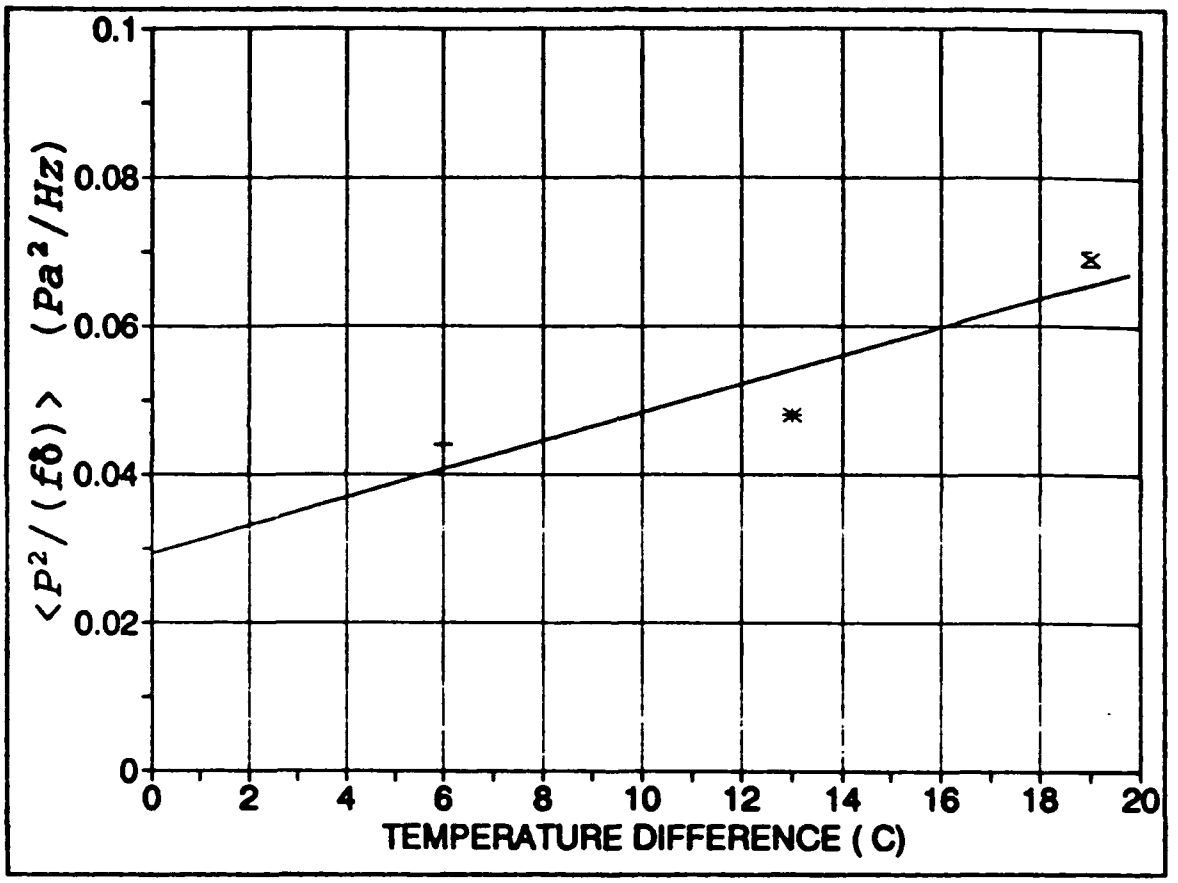

Figure 23. Average $P_d^2/f\delta$ versus temperature difference for bubbles produced from 4.25 mm raindrops.

VIII. CONCLUSION

The effects of temperature and salinity on the sound energy radiated from bubbles produced by raindrops, noted by Jacobus (1991), have been verified.

Salinity appears to decrease the sound energy produced by bubbles formed from small raindrops by as much as sixty percent. The damping constant is higher by an average of about ten percent which decreases the time the bubble oscillates. Secondly, increasing the salinity appears to decrease the dipole strength of the bubble thereby decreasing the total amount of energy radiated in accordance with (18).

In a study using large raindrops, which produce bubbles by the Type II mechanism, the absolute temperature difference between the drops and the surface of the water was found to have no affect on the damping constant. It did appear to effect the peak pressure of the bubble. As the absolute temperature between the drop and surface increased so did the dipole strength. This, in turn, ultimately would lead to increased radiation from bubbles when the absolute temperature difference is large.

APPENDIX A: CHANGE OF SLOPE IN THE BUBBLE DECAY SIGNAL

During the analysis of the bubble decay, eleven signals (out of 53) showed a change of the damping constant ("breaking point") during the active oscillation of the bubble. This is seen as a change of slope in the semi-log display in Figure 24. All eleven of these were Type 1 mechanisms, with five in fresh water and six in salt water. In all cases the change in slope was from small to large. The signal of each bubble showed no indications of spin-off bubbles which could affect the oscillation of these bubbles. Previous work (Medwin and Beaky,1989) attributes the change from large to small slope to non-linear oscillation (see also Longuet-Higgins,1992), whereas the change from small to large slope ("breaking point") is the result of a possible change in position (Medwin and Beaky,1989) or shape of the bubble as it oscillates (Strasberg,1953).

The signals of the bubbles were analyzed by measuring the period several times before and after the time at which the slope of the semi-log plot changed. These periods, which were measured at the baseline crossing (because of the tank related interference found in the peaks of many signals), were then used to obtain the bubble frequency. The change in frequency

before and after the "breaking point" was, for every bubble examined, small (between 0.59 and 2.12 percent of resonance frequency) if there was any change at all (three bubbles, two salt and one fresh, showed no frequency change). Of the bubbles which displayed a frequency change, two of them (one each in fresh and salt water) displayed an increase in frequency, while one fresh and one salt water bubble showed a decrease in frequency. Another four bubbles (two fresh and two salt water) displayed a pattern in which the frequency consistently varied between two closely related frequencies (a frequency difference never more than 2.11 percent of the resonance frequency) both before and after the "breaking point". The only possible difference between the fresh and salt water cases was that the fresh water bubbles usually displayed a larger frequency shift than the salt water bubbles.

Knowing that the frequency at which a bubble oscillates changes as it moves with respect to the water surface (increases as it moves towards the surface, decreases as it moves away) one possible explanation for a change in frequency at the "breaking point may be bubble movement (Medwin and Beaky, 1989). The change in frequency of an oscillating bubble can be related to its position with respect to the surface by:

$$F = \frac{1}{\sqrt{1-\left(\frac{a}{2z}\right)-\left(\frac{a}{2z}\right)^4}} \qquad (20)$$

(Strasberg,1953) where a is the bubble radius, z is the bubble depth and F is the ratio of the bubble frequencies before and after the "breaking point". Solving this equation for z showed that if the bubble were moving at all it was only minutely, on the order of a tenth of a millimeter. Using the fact that speed is equal to the distance travelled (roughly 0.1 mm) over time of travel (which in this case is the period of oscillation) would indicate that most of the bubbles are moving at speeds of one to two meters per second, which seems possible.

The damping constant was next analyzed before and after the "breaking point" for each bubble and these results compared to the corresponding change in frequency and to the theoretical damping constant for the frequencies (the change in frequency was small enough that both frequencies had the same theoretical damping constant). The results of these comparisons are shown in Table 2.

TABLE 2. CHANGE IN SLOPE OF DAMPING CONSTANT SUMMARY

SALT/FRESH	FREQUENCY 1	δ_1	FREQUENCY 2	δ_2	δ_{th}
SALT	10,818 Hz	.034	10,882 Hz	.057	.054
SALT	11,029 Hz	.025	11,029 Hz	.055	.055
SALT	11,029 Hz	.032	10,965 Hz	.055	.055
SALT	11,304 Hz	.036	11,304 Hz	.053	.056
SALT	11,556 Hz	.011	11,659 Hz	.058	.056
SALT	11,555 Hz	.022	11,555 Hz	.056	.056
FRESH	14,666 Hz	.033	14,915 Hz	.058	.060
FRESH	23,158 Hz	.046	23,158 Hz	.071	.071
FRESH	23,158 Hz	.033	22,759 Hz	.078	.071
FRESH	23,158 Hz	.044	23,036 Hz	.060	.071
FRESH	28,085 Hz	.074	28,696 Hz	.094	.076

In all cases, the damping constant increased with the final experimental value being closer to the theoretical value in all but one case. There was no evidence that the change in frequency and damping are related.

Another possible cause for the frequency variation could be a change from a spherical to a non-spherical shape (Strasberg,1953). This could explain the oscillation between two nearby frequencies as observed in four cases. An increased damping constant could also be one indication of increased radiation, and because a spherically shaped bubble radiates more effectively than an elliptical bubble, this

could indicate the bubble is changing from a non-spherical shape to a spherical shape (Strasberg,1953).

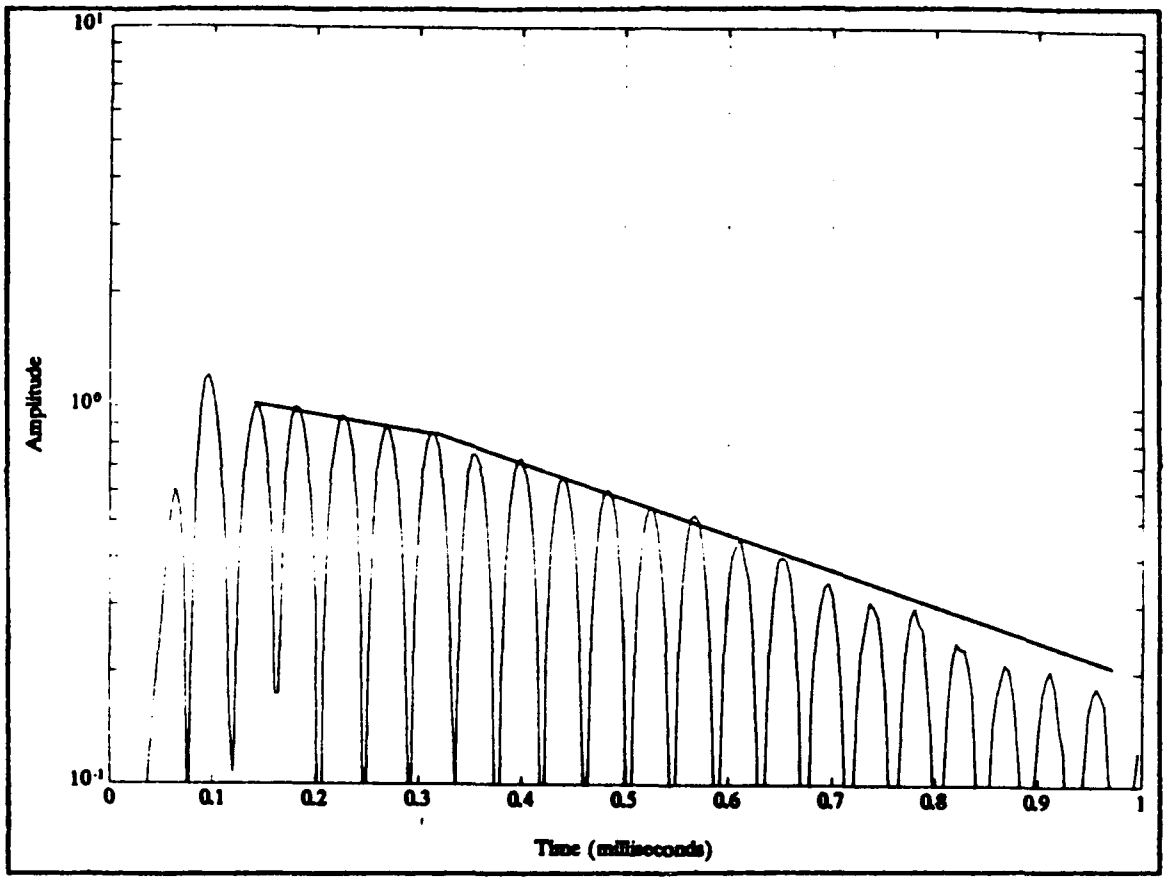

Figure 24. Semi-log plot of a bubble produced by a 0.985 mm drop falling at normal incidence to a salt water surface. This bubble is a good example of a oscillation with a "breaking point".

APPENDIX B: SECONDARY BUBBLES

Total sound energy produced by large raindrops increases as the temperature difference between drop and water surface increases (Jacobus,1991). One possible explanation for this increase is an increase in the number of secondary bubbles produced. These secondary bubbles, which have only been seen with Type II mechanisms, are either produced by the Type II mechanism itself (the downward jet) or by aerosols which are formed during the splash. Recent studies (Jacobus, 1991), have determined that the secondary bubbles oscillate at a higher frequency than the dominant bubble and with a smaller amplitude.

This study was conducted on the same bubbles produced by 4.2 mm drops in fresh water studied in Chapters Four, Six and Seven. The absolute temperature of the drops was varied to produce temperature differences of 6 and 19°C between the drop and surface (whose temperature was also changed). The signal of each bubble oscillation sampled by Computerscope was reviewed and the number of secondary bubbles was counted for each absolute temperature difference. As the temperature difference was increased, the rate of secondary bubble production increased from 48 percent (ΔT=6°C) to 54 percent

($\Delta T=19^{\circ}C$). This increase is not enough to explain the increase of sound energy from bubbles which is the result of the increase of absolute temperature difference between drop and surface.

Incidentally, Ostwald (1992) observed a secondary bubble production rate of 12 percent for 4.2 mm drops falling at normal incidence in salt water. This is significantly less than what was found in this study of 4.2 mm drops in fresh water.

REFERENCES

Clay, C.S. and Medwin, H., *Acoustical Oceanography*, Wiley, New York, 1977.

Devin, C.D., "Survey of thermal, radiation and viscous damping of pulsating air bubbles in water", *J. Acoust. Soc. Am.*, 31, pp. 1654-1667, 1959.

Elmore, P.A., Pumphrey, H.C. and Crum, L.A., "Further studies of the underwater noise produced by rainfall", Technical Report, National Center for Physical Acoustics, University of Mississippi, 38677, 1989.

Franz, G., "Splashes as sources of sounds in liquids", *J. Acoust. Soc. Am.*, 31, pp. 1080-1096, 1959.

Jacobus, P.W., "Underwater sound radiation from large raindrops", M.S. Thesis, Naval Postgraduate School, Monterey, CA, 93943, 1991.

Kinsler, L.E., Frey, A.R., Coppens, A.B. and Sanders, J.V., *Fundamentals Of Acoustics*, Wiley, 1982.

Longuet-Higgins, M.S., "Nonlinear damping of bubble oscillations by resonant interaction", *J. Acoust. Soc. Am.*, 91(3), pp. 1414-1422, 1992.

Medwin, H. and Beaky, M.M., "Bubble sources of the Knudsen sea noise spectra", *J. Acoust. Soc. Am.*, 86, pp. 1124-1130, 1989.

Medwin, H., Nystuen, J.A., Jacobus, P.A., Ostwald, L.H., Snyder, D.E., "The anatomy of underwater rain noise", to appear in *J. Acoust. Soc. Am. (1992)*.

Ostwald, L.H., "Predicting the underwater sound of moderate and heavy rainfall from laboratory measurements of radiation from single large water drops", M.S. Thesis, Naval Postgraduate School, Monterey, CA, 93940, 1992.

Pumphrey, H.C. and Crum, L.A., "Free oscillations of near-surface bubbles as a source of the underwater noise of rain", *J. Acoust. Soc. Am.*, 87(1), pp. 142-148, 1990.

Pumphrey, H.C., Crum, L.A. and Bjorno, L., "Underwater sound produced by individual drop impacts and rainfall", *J. Acoust. Soc. Am.*, 85(4), pp. 1518-1526, 1989.

Snyder, D.E., "Characteristics of sound radiation from large raindrops", M.S. Thesis, Naval Postgraduate School, Monterey, CA, 93940, 1990.

Strasberg, M., "Pulsation frequency of non spherical gas bubbles in liquids ", *J. Acoust. Soc. Am.*, 25, pp. 536-537, 1953.

INITIAL DISTRIBUTION LIST

		No. Copies
1.	Defense Technical Information Center Cameron Station Alexandria, VA 22304-6145	2
2.	Library, Code 52 Naval Postgraduate School Monterey, CA 93943-5002	2
3.	Department of Physics Attn: Professor H. Medwin, Code PH/Md Naval Postgraduate School Monterey, CA 93943	3
4.	Department of Physics Attn: Professor A.A. Atchley Naval Postgraduate School Monterey, CA 93943	2
5.	Department of Oceanography Attn: Professor J.A. Nystuen, Code OC/Ny Naval Postgraduate School Monterey, CA 93943	1
6.	Dr. Marshall Orr Office of Naval Research (Code 11250A) 800 N. Quincy Street Arlington, VA 22217	1
7.	LT Christopher Scofield 2427 Covington Rd Akron, OH 44313	2
8.	Mr. Harry Selsor Tactical Oceanography Warfare Support Office Bldg 1105, Room 102 Naval Research Laboratory Code 311 Stennis Space Center, MS, 39529-5004	1

9. LT Glenn Miller 1
Weapons Engineering Department UX11
Naval Postgraduate School
Monterey, CA 93943

10. LT Peter W. Jacobus 1
c/o Doroyhy Crain
116 Second St. Apt. 6
Pacific Grove, CA 93950

11. LT Leo H. Ostwald 1
Naval Submarine School
Code 80 SOAC Class 92050, Box 700
Groton, CT 06349-5700